Metabolic variables Blood was obtained from non-fasted mice between 15:00 and 17:00 hours. Blood glucose levels were determined by the glucose oxidase method using a reflectance glucometer (MS-GR102; Terumo, Tokyo, Japan) on days 0, 4, 7 and 14. Plasma insulin levels were measured by enzyme immunoassay with an Insulin-EIA kit (Morinaga, Tokyo, Japan). Plasma triacylglycerol, NEFA and total cholesterol levels were measured using enzymatic kits (Triglyceride E-test Wako, NEFA C-test Wako and Cholesterol E-test Wako, respectively; Wako Pure Chemicals, Osaka, Japan). Plasma leptin levels were determined using an RIA kit for mouse leptin (Linco Research Immunoassay, St Louis, MO, USA).

Glucose tolerance test (GTT) A GTT was performed on day 10. Mice were injected i.p. with 2.0 mg/g glucose after overnight fasting. Blood glucose and plasma insulin levels were measured at the indicated time points.

Liver and skeletal muscle triacylglycerol content Tissue triacylglycerol content was measured as described previously [7, 8], with modifications. Liver and quadriceps muscle were isolated at the end of the leptin infusion experiment, immediately frozen in liquid nitrogen and lipids extracted with isopropyl alcohol/heptane (1:1 vol./vol.). After evaporating the solvent, the lipids were resuspended in 99.5% (vol./vol.) ethanol, and the triacylglycerol content was measured using the Triglyceride E-test Wako kit.

Isoform-specific AMPK activity AMPK activity was determined as described previously [25, 26], with modifications. To measure α1 and α2 isoform-specific AMPK activity in skeletal muscle, AMPK was immunoprecipitated from muscle lysates (200 μg protein) with specific antibodies against the α1- and α2-subunits (Upstate Cell Signaling Solutions, Lake Placid, NY, USA) bound to Protein A-Sepharose beads, and the kinase activity of the immunoprecipitates was measured using 'SAMS' peptide and [γ-^{32}P]ATP.

Pair-feeding experiments STZ or STZ/HFD mice were fed the same amount of food consumed by the corresponding leptin-infused mice on the previous day, for 14 days. A GTT was performed on day 10 of the experiment. Liver and quadriceps muscle were obtained for triacylglycerol content measurements at the end of the pair-feeding experiment.

Statistical analyses Data are expressed as means±SEM. Comparison between or among groups was by Student's *t* test or ANOVA with Fisher's protected least significant difference test. $p<0.05$ was considered statistically significant.

Results

Generation of a mouse model of type 2 diabetes To generate a mouse model mimicking human type 2 diabetes with impaired insulin secretion and insulin resistance, we used low-dose STZ injection and HFD feeding. As shown in Table 1, HFD feeding effectively increased body weight, per cent body fat and plasma leptin levels in mice. With the development of adiposity, plasma insulin levels substan-

Table 1 Metabolic characteristics of the mouse model of type 2 diabetes

Variable	Mouse group			
	Control	HFD	STZ	STZ/HFD
Food intake (kJ/week)	329.0±9.3	350.7±20.0	365.3±15.1*	422.1±23.1**,†
Body weight (g)	26.8±0.6	34.4±1.3**	26.4±0.4	27.9±0.5†
Body fat (%)	19.8±0.7	40.6±1.1**	18.9±1.0	24.9±1.8*,†
Leptin (ng/ml)	4.7±0.6	26.4±1.0**	4.5±0.5	8.6±0.8**,††
Glucose (mmol/l)	8.3±0.2	9.2±0.4	17.5±2.3**	27.2±1.2**,††
Insulin (pmol/l)	160±28	315±71*	92±12*	160±38
Triacylglycerol (mmol/l)	0.66±0.09	0.86±0.08	1.11±0.14*	1.27±0.28*
NEFA (mEq/l)	0.77±0.06	1.08±0.09*	1.03±0.10*	0.99±0.09*
Total cholesterol (mmol/l)	1.48±0.08	3.61±0.18**	1.49±0.16	3.01±0.19**,††
Liver triacylglycerol content (mg/g tissue)	8.7±1.0	20.0±2.2**	10.2±0.9	27.1±1.7**,††
Skeletal muscle triacylglycerol content (mg/g tissue)	5.6±0.5	8.1±1.2*	5.4±0.5	7.8±0.8*,†

Values are means±SEM for 10–12 mice in each group
C57BL/6J mice were injected with vehicle and fed SD (control) or HFD, or injected with low-dose STZ and fed with SD (STZ) or HFD (STZ/HFD). Food intake for a week, body weight, per cent body fat, blood glucose levels and plasma levels for leptin, insulin, triacylglycerol, NEFA and total cholesterol were measured before the leptin infusion experiment. Blood samples were obtained during ad libitum feeding. Liver and skeletal muscle triacylglycerol contents were measured after the leptin infusion experiment
*$p<0.05$, **$p<0.01$ vs control mice; †$p<0.05$, ††$p<0.01$ vs STZ in STZ/HFD mice

tially increased, although blood glucose levels did not significantly increase, suggesting the development of insulin resistance. HFD feeding also increased plasma NEFA and total cholesterol levels, and liver and skeletal muscle triacylglycerol contents.

Low-dose STZ injection led to a substantial reduction of plasma insulin and hyperglycaemia in mice. Under these conditions, body weight, per cent body fat and plasma leptin levels were unchanged, although food intake was significantly increased. Low plasma insulin levels also led to an increase of plasma triacylglycerol and NEFA levels. Liver and skeletal muscle triacylglycerol contents were unchanged.

On the other hand, subsequent HFD feeding in low-dose STZ injected mice further increased food intake and moderately increased body weight, per cent body fat and plasma leptin levels even with the impairment of insulin secretion. Hyperglycaemia was exacerbated, although plasma insulin levels were mildly elevated, suggesting the development of insulin resistance. Increases of plasma triacylglycerol, NEFA and total cholesterol levels, and liver and skeletal muscle triacylglycerol contents, were also observed in these STZ/HFD mice.

Since STZ/HFD mice manifested increased adiposity and disorders in glucose and lipid metabolism accompanied by impaired insulin secretion and insulin resistance, we used STZ/HFD mice as a model of type 2 diabetes with increased adiposity in the present study.

Effect of leptin on food intake and body weight As shown in Fig. 1a, continuous leptin infusion elevated plasma leptin levels from baseline almost equally in control, HFD, STZ and STZ/HFD mice. Under these conditions, food intake was significantly suppressed in control, STZ and STZ/HFD mice, while that in HFD was unchanged (Fig. 1b). Consistent with food intake, body weight was effectively decreased in control, STZ and STZ/HFD mice, while that in HFD mice was unchanged (Fig. 1c).

Effect of leptin on glucose metabolism In control mice, leptin infusion did not affect blood glucose levels during ad libitum feeding but markedly decreased plasma insulin levels, suggesting the enhancement of insulin sensitivity (Fig. 2a, e). In HFD mice, leptin infusion showed no effect on either blood glucose levels or plasma insulin levels (Fig. 2b, e). On the other hand, both blood glucose levels and plasma insulin levels were effectively decreased after 2 weeks of leptin infusion in STZ and STZ/HFD mice, suggesting the improvement of insulin sensitivity (Fig. 2c–e).

To further evaluate the effect of leptin on glucose metabolism, we performed i.p. GTTs (Fig. 3). In control, STZ and STZ/HFD mice, leptin infusion significantly improved glucose tolerance with reduction of plasma insulin levels not only in the fasting state but also after the glucose load, suggesting an improvement of insulin sensitivity. In contrast, in HFD mice, leptin infusion did not improve glucose tolerance and also did not suppress plasma insulin levels before or after glucose load.

Effect of leptin on plasma lipid profiles Leptin infusion did not affect plasma triacylglycerol, NEFA and total cholesterol levels in control mice (Fig. 4a–c). Leptin infusion also did not change plasma triacylglycerol, NEFA and total cholesterol levels in HFD mice, even though basal plasma NEFA and total cholesterol levels were elevated. In STZ mice, leptin infusion effectively decreased plasma triacylglycerol and NEFA levels, which were elevated at baseline, while leptin infusion did not affect plasma total cholesterol levels, which were not elevated at baseline. In STZ/HFD

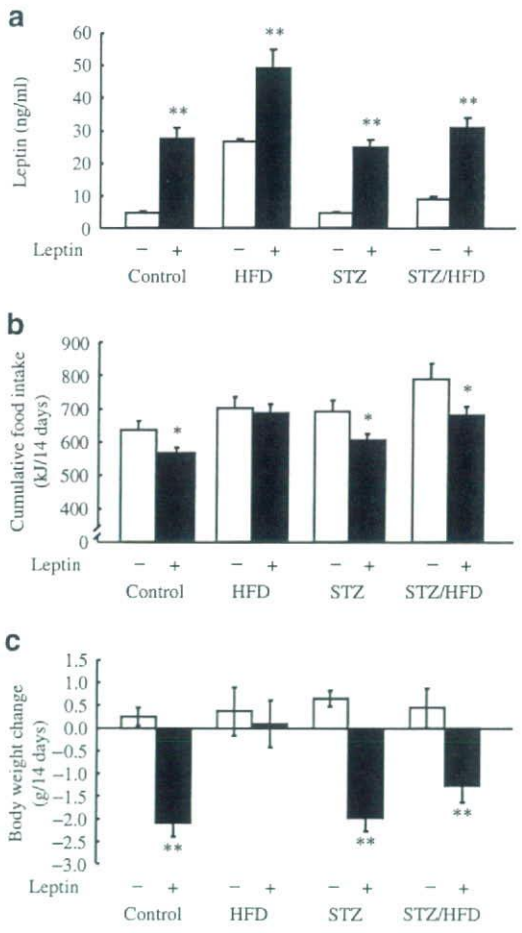

Fig. 1 Effect of leptin on leptin levels, food intake and body weight. Leptin levels on day 14 (**a**), cumulative food intake (**b**) and change in body weight (**c**) after 14 days of leptin infusion in control, HFD, STZ and STZ/HFD mice. Values are means±SEM (n=10–17). *p<0.05, **p<0.01 vs corresponding saline-infused mice

mice, leptin infusion also effectively decreased plasma triacylglycerol, NEFA and total cholesterol levels, which were elevated at baseline.

Effect of leptin on liver and skeletal muscle triacylglycerol contents To assess whether the improvement of glucose metabolism by leptin infusion was associated with the reduction of triacylglycerol content in insulin-target tissues, we examined the effect of leptin infusion on liver and skeletal muscle triacylglycerol contents. As shown in Fig. 5, leptin infusion apparently decreased triacylglycerol contents of both liver and skeletal muscle in control, STZ and STZ/HFD mice, in which glucose metabolism was improved by leptin infusion. In contrast, leptin infusion decreased triacylglycerol content of neither liver nor skeletal muscle in HFD mice, in which glucose metabolism was unchanged by leptin infusion.

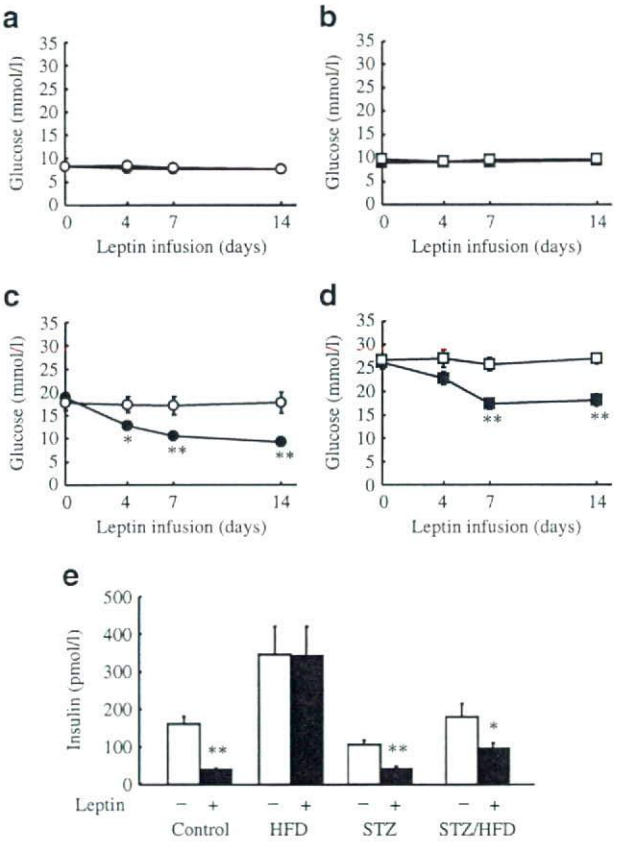

Fig. 2 Effect of leptin infusion for 14 days on blood glucose and plasma insulin levels during ad libitum feeding. Blood glucose levels on days 0, 4, 7 and 14 in control (**a**), HFD (**b**), STZ (**c**) and STZ/HFD mice (**d**). White symbols, saline-infused; black symbols, leptin-infused. **e** Plasma insulin levels during ad libitum feeding on day 14 in control, HFD, STZ and STZ/HFD mice. Values are means±SEM (n=10–17). *p<0.05, **p<0.01 vs corresponding saline-infused mice

Effect of leptin on AMPK activity in skeletal muscle Leptin infusion did not affect α1 isoform-specific AMPK activity in skeletal muscle in any group of mice (Fig. 6a). On the other hand, leptin infusion significantly increased α2 isoform-specific AMPK activity in skeletal muscle in control, STZ and STZ/HFD mice (Fig. 6b). However, no significant increase of α2 AMPK activity in skeletal muscle was observed in HFD mice.

Pair-feeding experiments We investigated whether the reduction of food intake by leptin infusion is the reason

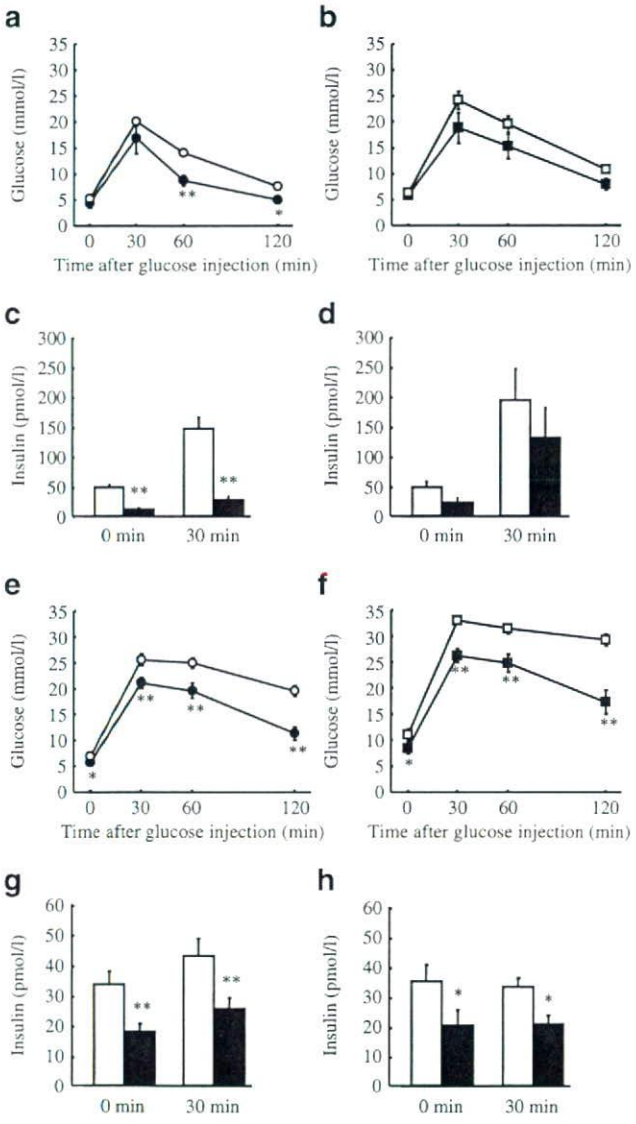

Fig. 3 Effect of leptin on glucose tolerance and insulin secretion during GTTs. Blood glucose and plasma insulin levels were measured at the indicated time points in control (**a, c**), HFD (**b, d**), STZ (**e, g**) and STZ/HFD mice (**f, h**). Values are means±SEM (n=10–17). *p<0.05, **p<0.01 vs corresponding saline-infused mice

for its efficacy in improving glucose metabolism. We pair-fed STZ and STZ/HFD mice the same amount of food consumed by the corresponding leptin-infused mice on the previous day. Pair-feeding did not improve glucose tolerance in GTTs in STZ and STZ/HFD mice (data not shown). Moreover, when compared with basal values (Table 1), no significant decrease of liver and skeletal muscle triacylglycerol contents was observed in pair-fed STZ and STZ/HFD mice (liver triacylglycerol content: 8.3±1.2 and 30.0±5.6 mg/g tissue; skeletal muscle triacylglycerol content: 5.4±0.5 and 6.6±0.5 mg/g tissue, in pair-fed STZ and STZ/HFD mice, respectively, $n=5$ in each group of mice), in contrast to the corresponding leptin-infused mice (Fig. 5).

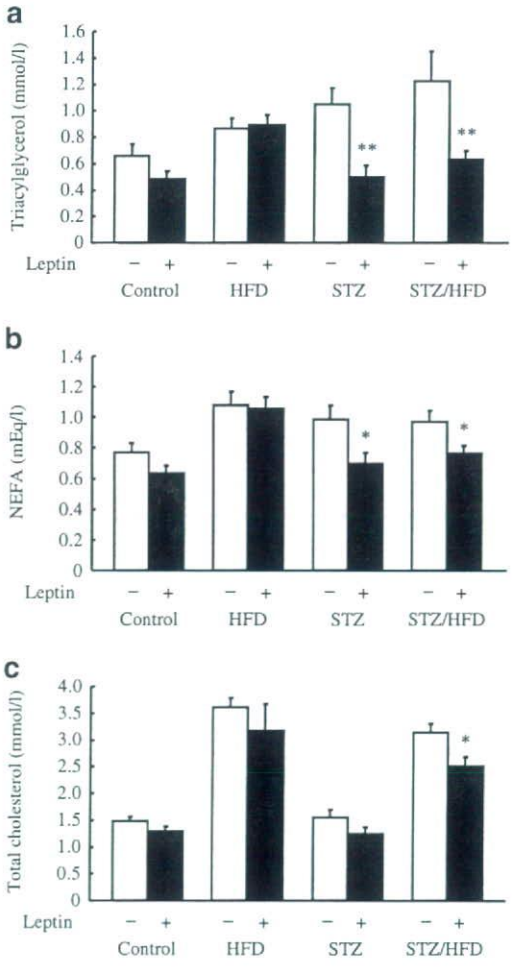

Fig. 4 Effect of leptin on plasma lipid profiles. Plasma triacylglycerol (**a**), NEFA (**b**) and total cholesterol levels (**c**) during ad libitum feeding on day 14 in control, HFD, STZ and STZ/HFD mice. Values are means±SEM ($n=10$–17). *$p<0.05$, **$p<0.01$ vs corresponding saline-infused mice

Discussion

The effectiveness of leptin treatment in diabetes has been reported in patients with leptin deficiency and lipodystrophy and in amenorrhoea in patients with hypothalamic hypogonadism caused by low body weight [5, 13–16, 27]. These patients are in hypoleptinaemic states, and hypoleptinaemia is involved in the pathophysiology of their diseases. However, whether leptin treatment is effective in normo- or hyperleptinaemic states has not been fully examined. The aim of the present study was to explore the therapeutic usefulness of leptin in type 2 diabetes, which is often accompanied by increased adiposity. Type 2 diabetes develops as a result of insulin resistance in target tissues and impaired insulin secretion, accompanied by increased adiposity. To generate a mouse model mimicking human type 2 diabetes, we used a combination of low-dose STZ and HFD. Although high-dose STZ injection generally reduces body weight, with a marked reduction of insulin levels [16], low-dose STZ used in this study did not reduce body weight. In addition, subsequent HFD feeding in low-dose STZ injected mice could increase body weight even

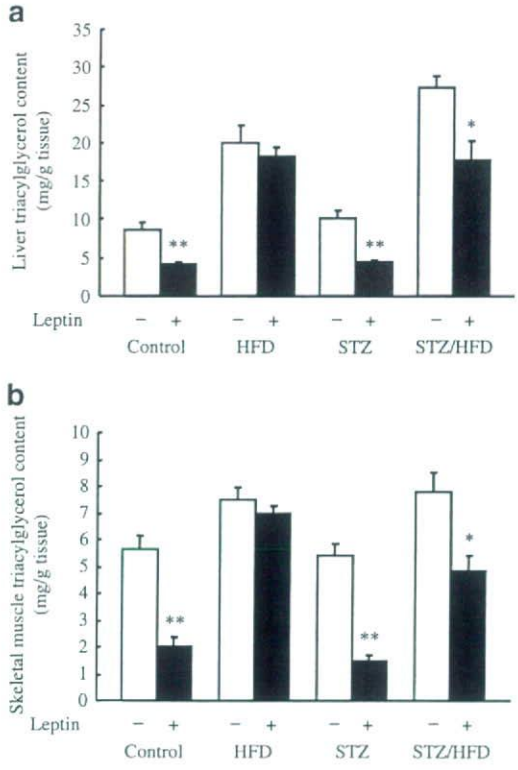

Fig. 5 Effect of leptin on liver and skeletal muscle triacylglycerol contents. Liver (**a**) and skeletal muscle (**b**) triacylglycerol contents on day 14 in STZ and STZ/HFD mice. Values are means±SEM ($n=10$–13). *$p<0.05$, **$p<0.01$ vs corresponding saline-infused mice

with the impairment of insulin secretion in this study. Consistent with the increase in body weight and per cent body fat, STZ/HFD mice showed a nearly twofold increase in plasma leptin levels compared with control mice (Table 1). In humans, plasma leptin levels positively correlated with BMI, and a twofold increase in plasma leptin levels corresponds to a BMI in the range of 25–30 kg/m^2 [28, 29]. According to recent clinical studies, the average BMI in patients with type 2 diabetes is within this overweight range [30–32]. HFD mice showed a larger increase in adiposity and plasma leptin levels than did STZ/HFD mice. However, unlike STZ/HFD mice, HFD mice did not develop hyperglycaemia, because of compensatory hyperinsulinaemia. Therefore, we used STZ/HFD mice as an appropriate model to examine the efficacy of leptin in type 2 diabetes with increased adiposity.

The present study showed that the effect of leptin on food intake and body weight was attenuated in obese HFD mice (Fig. 1b, c). In general, in human obesity and rodent models of diet-induced obesity, even though leptin levels rise proportionally with adiposity, the increased leptin fails to suppress the progression of obesity. Moreover, obese humans and rodents are weakly responsive to exogenously administered leptin in terms of body weight reduction

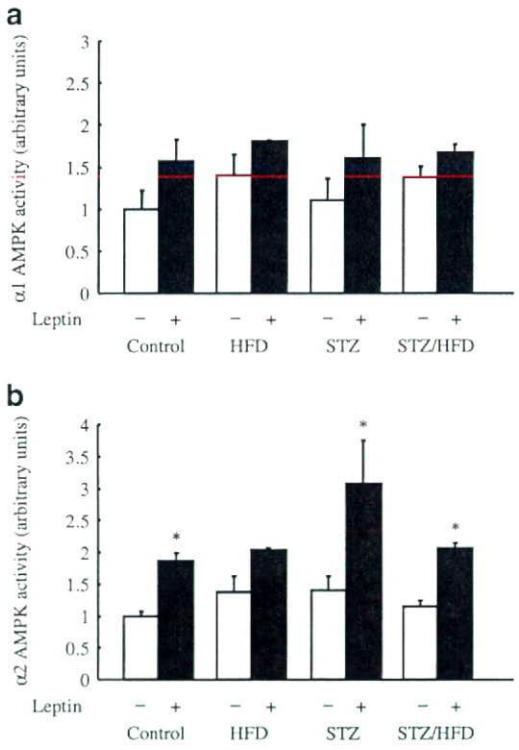

Fig. 6 Effect of leptin on isoform-specific AMPK activity in skeletal muscle. α1 AMPK activity (**a**) and α2 AMPK activity (**b**) on day 14 in soleus muscle of STZ and STZ/HFD mice. Values are means±SEM (n=4–5). *p<0.05 vs corresponding saline-infused mice

[33, 34]. This leptin ineffectiveness is called leptin resistance. The present study also showed that the effect of leptin on glucose and lipid metabolism was attenuated in obese HFD mice (Figs 2, 3, 4 and 5). In contrast, even under HFD feeding, leptin effectively improved glucose and lipid metabolism in STZ/HFD mice. Impaired insulin secretion caused by STZ injection could reduce the effect of HFD feeding on the development of obesity in STZ/HFD mice. As a result, leptin resistance could be mild, if any, in STZ/HFD mice. The present study demonstrated that leptin could be a glucose-lowering drug for the treatment of type 2 diabetes with impaired insulin secretion.

Fat accumulation in insulin target tissues is considered to be one of the causes of insulin resistance, and is called lipotoxicity [35, 36]. Indeed, HFD and STZ/HFD mice exhibited insulin resistance and increased liver and skeletal muscle triacylglycerol contents (Table 1). In the present study, we investigated an association between the improvement of glucose metabolism by leptin infusion and the reduction of liver and skeletal muscle triacylglycerol contents. Leptin infusion enhanced insulin sensitivity in control, STZ and STZ/HFD mice, in which it decreased liver and skeletal muscle triacylglycerol contents (Figs 3 and 5). In contrast, leptin infusion did not improve insulin resistance in HFD mice, in which it did not decrease liver and skeletal muscle triacylglycerol contents. Moreover, pair-feeding neither improved glucose tolerance nor decreased the liver and skeletal muscle triacylglycerol contents in STZ and STZ/HFD mice. These results suggest that the improvement of glucose metabolism by leptin infusion is associated with a reduction in liver and skeletal muscle triacylglycerol contents.

Leptin has been shown to selectively stimulate activation of the α2 catalytic subunit of AMPK in skeletal muscle [37]. AMPK is a key enzyme that mediates the leptin effect on fatty acid β-oxidation in skeletal muscle. In the present study, leptin infusion effectively decreased skeletal muscle triacylglycerol content in control, STZ and STZ/HFD mice (Fig. 5b), in which it increased α2 AMPK activity in skeletal muscle (Fig. 6b). In contrast, leptin infusion did not decrease skeletal muscle triacylglycerol content in HFD mice (Fig. 5b), in which it did not increase α2 AMPK activity in skeletal muscle (Fig. 6b). Increased fatty acid β-oxidation through α2 AMPK activation in skeletal muscle is considered to be one of the mechanisms by which leptin decreases skeletal muscle triacylglycerol content [9].

The present study also showed that leptin infusion effectively improved hyperlipidaemia in STZ and STZ/HFD mice (Fig. 4). Increased lipoprotein lipase activity, increased clearance of triacylglycerol [7], reduction of triacylglycerol synthesis by controlling key transcription factors [38] and increased energy expenditure through fatty acid β-oxidation have been reported as mechanisms by

which leptin decreases plasma triacylglycerol levels. The present study demonstrated activation of α2 AMPK activity by leptin infusion in skeletal muscle (Fig. 6b), which might contribute to increased energy expenditure in our leptin-infused STZ and STZ/HFD mice. It is also well known that impaired insulin action induces hyperlipidaemia [39]. It is also possible that leptin improved hyperlipidaemia by enhancement of insulin sensitivity in the present study.

The present study demonstrated that pair-feeding neither improved glucose tolerance nor decreased liver and skeletal muscle triacylglycerol contents in STZ and STZ/HFD mice. Previously, we and others have demonstrated that food intake reduction alone was insufficient for improving glucose and lipid metabolism [6, 10, 12]. It has also been reported that fasting insulin and triacylglycerol levels increased within several days after withdrawal of leptin administration even though the level of food intake remained constant in the patients with lipodystrophy [13]. Furthermore, it has been demonstrated that leptin administration decreases liver and skeletal muscle triacylglycerol contents in patients with lipodystrophy [40]. These results indicate that leptin improves glucose and lipid metabolism independently of the food intake reduction.

With the dose of leptin used in the present study, the plasma leptin levels in STZ/HFD mice increased to the levels of obese HFD mice (mean leptin levels in leptin-infused STZ/HFD mice, 30.8 ng/ml) (Fig. 1a), which can be seen in human obese individuals. In our clinical research on leptin-replacement therapy in patients with generalised lipodystrophy, the peak plasma leptin levels of the 400% dose under the protocol of once-daily injections was 34.5± 2.1 (mean±SE) ng/ml, and the therapy was well tolerated without any adverse effects for about 5 years [15]. In addition, higher leptin levels were obtained in the obese human clinical trial [33]. Therefore, the leptin levels achieved with the dose used in the present study could be clinically applied in humans.

In conclusion, the present study demonstrates that leptin therapy improves glucose and lipid metabolism and enhances insulin sensitivity in a mouse model of type 2 diabetes with an overweight range of adiposity. Our findings indicate that leptin could be a new glucose-lowering drug for the treatment of type 2 diabetes in humans.

Acknowledgements We thank M. Nagamoto for technical assistance and Y. Koyama for secretarial assistance. This work was supported in part by research grants from the Ministry of Education, Culture, Sports, Science and Technology of Japan; the Ministry of Health, Labour and Welfare of Japan; the Takeda Medical Research Foundation and Japan Foundation of Applied Enzymology; and the ONO Medical Research Foundation.

Duality of interest The authors declare that there is no duality of interest associated with this manuscript.

References

1. Halaas JL, Gajiwala KS, Maffei M (1995) Weight-reducing effects of the plasma protein encoded by the obese gene. Science 269:543–546
2. Friedman JM, Halaas JL (1998) Leptin and the regulation of body weight in mammals. Nature 395:763–770
3. Muzzin P, Eisensmith RC, Copeland KC, Woo SLC (1996) Correction of obesity and diabetes in genetically obese mice by leptin gene therapy. Proc Natl Acad Sci U S A 93:14804–14808
4. Montague CT, Farooqi IS, Whitehead JP (1997) Congenital leptin deficiency is associated with severe early-onset obesity in humans. Nature 387:903–908
5. Licinio J, Caglayan S, Ozata M (2004) Phenotypic effects of leptin replacement on morbid obesity, diabetes mellitus, hypogonadism, and behavior in leptin-deficient adults. Proc Natl Acad Sci U S A 101:4531–4536
6. Ogawa Y, Masuzaki H, Hosoda K (1999) Increased glucose metabolism and insulin sensitivity in transgenic skinny mice overexpressing leptin. Diabetes 48:1822–1829
7. Matsuoka N, Ogawa Y, Masuzaki H (2001) Decreased triglyceride-rich lipoproteins in transgenic skinny mice overexpressing leptin. Am J Physiol Endocrinol Metab 280:E334–E339
8. Tanaka T, Masuzaki H, Yasue S (2007) Central melanocortin signaling restores skeletal muscle AMP-activated protein kinase phosphorylation in mice fed a high-fat diet. Cell Metabolism 5:395–402
9. Tanaka T, Hidaka S, Masuzaki H (2005) Skeletal muscle AMP-activated protein kinase phosphorylation parallels metabolic phenotype in leptin transgenic mice under dietary modification. Diabetes 54:2365–2374
10. Ebihara K, Ogawa Y, Masuzaki H (2001) Transgenic overexpression of leptin rescues insulin resistance and diabetes in a mouse model of lipoatrophic diabetes. Diabetes 50:1440–1448
11. Miyanaga F, Ogawa Y, Ebihara K (2003) Leptin as an adjunct of insulin therapy in insulin-deficient diabetes. Diabetologia 46:1329–1337
12. Shimomura I, Hammer RE, Ikemoto S, Brown MS, Goldstein JL (1999) Leptin reverses insulin resistance and diabetes mellitus in mice with congenital lipodystrophy. Nature 401:73–76
13. Oral EA, Simha V, Ruiz E (2002) Leptin-replacement therapy for lipodystrophy. N Engl J Med 346:570–578
14. Ebihara K, Masuzaki H, Nakao K (2004) Long-term leptin-replacement therapy for lipoatrophic diabetes. N Engl J Med 351:615–616
15. Ebihara K, Kusakabe T, Hirata M (2007) Efficacy and safety of leptin-replacement therapy and possible mechanisms of leptin actions in patients with generalized lipodystrophy. J Clin Endocrinol Metab 92:532–541
16. Beltrand J, Beregszaszi M, Chevenne D (2007) Metabolic correction induced by leptin replacement treatment in young children with Berardinelli–Seip congenital lipoatrophy. Pediatrics 120:e291–e296
17. Taylor SI (1999) Deconstructing type 2 diabetes. Cell 97:9–12
18. Ishii M, Yoshioka Y, Ishida W (2005) Liver fat content measured by magnetic resonance spectroscopy at 3.0 tesla independently correlates with plasminogen activator inhibitor-1 and body mass index in type 2 diabetic subjects. Tohoku J Exp Med 206:23–30
19. Sinha R, Dufour S, Petersen KF (2002) Assessment of skeletal muscle triglyceride content by ^{1}H nuclear magnetic resonance spectroscopy in lean and obese adolescents: relationships to insulin sensitivity, total body fat, and central adiposity. Diabetes 51:1022–1027
20. Kiess W, Anil M, Blum WF (1998) Serum leptin levels in children and adolescents with insulin-dependent diabetes mellitus in relation to metabolic control and body mass index. Eur J Endocrinol 138:501–509

21. Ding SY, Shen ZF, Chen YT, Sun SJ, Liu Q, Xie MZ (2005) Pioglitazone can ameliorate insulin resistance in low-dose streptozotocin and high sucrose-fat diet induced obese rats. Acta Pharmacol Sin 26:575–580
22. Luo J, Quan J, Tsai J (1998) Nongenetic mouse models of non-insulin-dependent diabetes mellitus. Metabolism 47:663–668
23. Mu J, Woods J, Zhou YP (2006) Chronic inhibition of dipeptidyl peptidase-4 with a sitagliptin analog preserves pancreatic β-cell mass and function in a rodent model of type 2 diabetes. Diabetes 55:1695–1704
24. Shertzer HG, Schneider SN, Kendig EL, Clegg DJ, D'Alessio DA, Genter MB (2008) Acetaminophen normalizes glucose homeostasis in mouse models for diabetes. Biochem Pharmacol 75:1402–1410
25. Miyamoto L, Toyoda T, Hayashi T (2007) Effect of acute activation of 5′-AMP-activated protein kinase on glycogen regulation in isolated rat skeletal muscle. J Appl Physiol 102:1007–1013
26. Toyoda T, Tanaka S, Ebihara K (2006) Low-intensity contraction activates the alpha1-isoform of 5′-AMP-activated protein kinase in rat skeletal muscle. Am J Physiol Endocrinol Metab 290:E583–E590
27. Welt CK, Chan JL, Bullen J (2004) Recombinant human leptin in women with hypothalamic amenorrhea. N Engl J Med 351:987–997
28. Buettner R, Bollheimer LC, Zietz B (2002) Definition and characterization of relative hypo- and hyperleptinemia in a large Caucasian population. J Endocrinol 175:745–756
29. Peltz G, Sanderson M, Pérez A, Sexton K, Ochoa Casares D, Fadden MK (2007) Serum leptin concentration, adiposity, and body fat distribution in Mexican–Americans. Arch Med Res 38:563–570
30. Widjaja A, Stratton IM, Horn R, Holman RR, Tuner R, Brabant G (1997) UKPDS 20: Plasma leptin, obesity, and plasma insulin in type 2 diabetic subjects. J Clin Endocrinol Metab 82:654–657
31. Sone H, Yoshimura Y, Tanaka S (2007) Cross-sectional association between BMI, glycemic control and energy intake in Japanese patients with type 2 diabetes. Analysis from the Japan Diabetes Complications Study. Diabetes Res Clin Pract 77S:S23–S29
32. Sone H, Ito H, Ohashi Y, Akanuma Y, Yamada N, Japan Diabetes Complications Study (JDCS) Group (2003) Obesity and type 2 diabetes in Japanese patients. Lancet 361:85
33. Heymsfield SB, Greenberg AS, Fujioka K (1999) Recombinant leptin for weight loss in obese and lean adults: a randomized, controlled, dose-escalation trial. JAMA 282:1568–1575
34. El-Haschimi K, Pierroz DD, Hileman SM, Bjorbaek C, Flier JS (2000) Two defects contribute to hypothalamic leptin resistance in mice with diet-induced obesity. J Clin Invest 105:1827–1832
35. Schulman GI (2000) Cellular mechanisms of insulin resistance. J Clin Invest 106:171–176
36. Unger RH (2003) Minireview: Weapons of lean body mass destruction: the role of ectopic lipids in the metabolic syndrome. Endocrinology 144:5159–5165
37. Minokoshi Y, Kim YB, Peroni OD (2002) Leptin stimulates fatty-acid oxidation by activating AMP-activated protein kinase. Nature 415:339–343
38. Cohen P, Miyazaki M, Socci ND (2002) Role for stearoyl-CoA desaturase-1 in leptin-mediated weight loss. Science 297:240–243
39. Reaven GM (2005) Why Syndrome X? From Harold Himsworth to the insulin resistance syndrome. Cell Metab 1:9–14
40. Petersen KF, Oral EA, Dufour S (2002) Leptin reverses insulin resistance and hepatic steatosis in patients with severe lipodystrophy. J Clin Invest 109:1345–1350

FEBS Letters 583 (2009) 1029–1033

FEBS Letters

journal homepage: www.FEBSLetters.org

Adipogenic differentiation of human induced pluripotent stem cells: Comparison with that of human embryonic stem cells

Daisuke Taura [a,1], Michio Noguchi [a,1], Masakatsu Sone [a,*], Kiminori Hosoda [a,*], Eisaku Mori [a], Yohei Okada [b], Kazutoshi Takahashi [c,d], Koichiro Homma [a,e], Naofumi Oyamada [a], Megumi Inuzuka [a], Takuhiro Sonoyama [a], Ken Ebihara [a], Naohisa Tamura [a], Hiroshi Itoh [e], Hirofumi Suemori [f], Norio Nakatsuji [g,h], Hideyuki Okano [b], Shinya Yamanaka [c,d], Kazuwa Nakao [a]

[a] Department of Medicine and Clinical Science, Kyoto University Graduate School of Medicine, 54 Shogoin Kawahara-cho, Sakyo-ku, Kyoto 606-8507, Japan
[b] Department of Physiology, Keio University, School of Medicine, Tokyo, Japan
[c] Department of Stem Cell Biology, Institute for Frontier Medical Sciences, Kyoto University, Kyoto, Japan
[d] Center for iPS Cell Research and Application (CiRA), Institute for Integrated Cell-Material Sciences, Kyoto, Japan
[e] Department of Internal Medicine, Keio University School of Medicine, Tokyo, Japan
[f] Laboratory of Embryonic Stem Cell Research, Stem Cell Research Center, Institute for Frontier Medical Sciences, Kyoto University, Kyoto, Japan
[g] Department of Development and Differentiation, Institute for Frontier Medical Sciences, Kyoto University, Kyoto, Japan
[h] Institute for Integrated Cell-Material Sciences (iCeMS), Kyoto University, Kyoto, Japan

ARTICLE INFO

Article history:
Received 28 December 2008
Revised 10 February 2009
Accepted 21 February 2009
Available online 27 February 2009

Edited by Robert Barouki

Keywords:
Adipogenesis
Adipocyte
Stem cell
Differentiation

ABSTRACT

Induced pluripotent stem (iPS) cells were recently established from human fibroblasts. In the present study we investigated the adipogenic differentiation properties of four human iPS cell lines and compared them with those of two human embryonic stem (ES) cell lines. After 12 days of embryoid body formation and an additional 10 days of differentiation on Poly-L-ornithine and fibronectin-coated dishes with adipogenic differentiation medium, human iPS cells exhibited lipid accumulation and transcription of adipogenesis-related molecules such as C/EBPα, PPARγ2, leptin and aP2. These results demonstrate that human iPS cells have an adipogenic potential comparable to human ES cells.

1. Introduction

Pluripotent embryonic stem (ES) cells have been considered potent candidates for regenerative medicine as an unlimited source of cells for the transplantation therapy and a useful tool for the investigation of cell development/differentiation, especially after establishment of human ES cells [1]. We previously clarified the differentiation process of mouse, monkey and human ES cells into vascular cells [2–4] and demonstrated that transplantation of vascular cells derived from human ES cells may constitute a novel strategy for vascular regeneration [4,5]. A number of immunological and ethical problems remain to be overcome before clinical application of the ES cells, however. Recently, novel ES cell-like pluripotent cells, termed induced pluripotent stem (iPS) cells, were generated by introducing four transcription factors (Oct3/4, Sox2, Klf4 and c-Myc) into mouse skin fibroblasts [6], and soon thereafter iPS cells were also generated from human skin fibroblasts [7,8]. Since then, a new generation of human iPS cells has been generated by introducing into fibroblasts just three of the aforementioned transcription factors (c-Myc was omitted) [9]. By overcoming the immunological and ethical problems associated with ES cells, iPS cells open a new avenue for cell transplantation-based regenerative medicine and provide a powerful new tool with which to investigate organ development/differentiation in specific disease states, especially in inherited diseases.

Generalized lipodystrophy consists of congenital and acquired types characterized by the lack of the whole adipose tissue, which leads to severe insulin-resistant diabetes, hypertriglyceridemia and fatty liver. We previously analyzed genes and phenotypes of congenital generalized lipodystrophic Japanese [10] and also demonstrated the long-lasting efficacy and safety of the leptin-replacement therapy in these patients [11–13]. Since metabolic abnormality in the mouse model is known to be cured by mature

* Corresponding authors. Fax: +81 75 771 9452.
E-mail addresses: sonemasa@kuhp.kyoto-u.ac.jp (M. Sone), kh@kuhp.kyoto-u.ac.jp (K. Hosoda).
[1] These authors contributed equally to this work.

0014-5793/$36.00 © 2009 Federation of European Biochemical Societies. Published by Elsevier B.V. All rights reserved.
doi:10.1016/j.febslet.2009.02.031

adipocytes transplantation, the regeneration therapy of the adipose tissue with human iPS cells-derived adipocytes is the ideal goal for lipodystrophic patients. Moreover, in vitro adipogenic differentiation system of human iPS cells will contribute to elucidate the pathogenesis of congenital generalized lipodystrophy when iPS cell lines are established from patients with lipodystrophy. In the present study we have investigated the adipogenic differentiation of human iPS cells and compared with that of human ES cells.

2. Materials and methods

2.1. Cells and culture

Four human iPS cell lines (201B6, 201B7, 253G1 and 253G4) were investigated. The 201B6 (B6) and 201B7 (B7) lines were generated by introducing four transcription factors (Oct3/4, Sox2, Klf4 and c-Myc) into human skin fibroblasts while the 253G1 (G1) and 253G4 (G4) lines were generated using only three factors (c-Myc was omitted) [9]. These iPS cell lines were maintained as previously described [7]. Two human ES cell lines (H9 and KhES-1) were used and maintained as previously described [1,14].

2.2. Adipogenic differentiation

For embryoid body (EB) formation, iPS and ES colonies were digested with 1 mg/ml collagenase type IV (GIBCO, CA, USA) and plated onto non-adherent bacterial culture dishes, where they were allowed to aggregate in maintenance medium without bFGF. Retinoic acid (Sigma–Aldrich, Japan) was added to the medium to a concentration of 100 nM from day 2 to day 5. After 12 days, EBs were transferred to 6-well plates coated with a combination of 30 μg/ml Poly-L-ornithine (Sigma–Aldrich) and 2 μg/ml fibronectin (Sigma–Aldrich). To induce adipocyte differentiation from iPS and ES cells, we applied a modification of a procedure described previously for use with mouse and human ES cells (Fig. 1) [15–19]. Differentiation was induced for 10 days using medium consisting of DMEM-F12, 10% KSR, and an adipogenic cocktail (0.5 mM IBMX, 0.25 μM dexamethasone, 1 μg/ml insulin, 0.2 mM indomethacin and 1 μM pioglitazone).

2.3. Immunocytochemistry

Immunocytochemistry was carried out as previously described [7]. The anti-human primary antibodies included Nanog (R&D Systems, MN, USA) and Alexa 488-conjugated SSEA-4 (Santa Cruz Biotechnology Inc., CA, USA) and TRA1-60 (CHEMICON, LA, USA). The TRA1-60 antibody was labeled using an Alexa Fluor 488 Monoclonal Antibody Labeling Kit (Molecular Probes, OR, USA). Alexa 546-conjugated donkey anti-sheep IgG (Molecular Probes, OR, USA) served as the secondary antibody. Alkaline phosphatase activity was detected using a BCIP/NBT substrate system (Dakocytomation, CA, USA).

2.4. Oil Red O staining and microscopic analysis of adipocytes

Cells were washed with phosphate-buffered saline (PBS) twice, fixed in 3.7% formaldehyde for 1 h and then stained with 0.6% (w/v) Oil Red O (Nacalai Tesque, Japan) solution (60% isopropanol, 40% water) for 2 h at room temperature. The cells were then washed with water to remove unbound dye. Subsequently, the bound Oil Red O was eluted with isopropanol.

After staining with Oil Red O, each EB was examined microscopically for the presence of adipocyte colonies, and the percentage of EBs with outgrowths showing adipocyte positivity was determined as previously described [15]. EBs in which adipocytes accounted for more than half of their circumference were considered adipocyte-positive. The percent area of Oil Red O staining (+) was determined at 20× magnification by counting the number of pixels exhibiting Oil Red O positivity in selected microscope fields (449 × 338 pixels). Four randomly selected fields were examined in each well of a 6-well plate, and the percent area was calculated as the average for the four fields. Six independent experiments were performed for each cell line.

Table 1
Primers for reverse-transcription polymerase chain reaction.

Gene		Sequence
Nanog	Sense	CAGCCCCGATTCTTCCACCAGTCCC
	Antisense	CGGAAGATTCCCAGTCGGGTTCACC
PPARγ2	Sense	ATTGACCCAGAAAGCGATTC
	Antisense	CAAAGGAGTGGGAGTGGTCT
C/EBPα	Sense	GCAAACTCACCGCTCCAATG
	Antisense	TTAGGTTCCAAGCCCCAAGTC
aP2	Sense	AACCTTAGATGGGGGTGTCCTG
	Antisense	TCGTGGAAGTGACGCCTTTC
Leptin	Sense	GAACCCTGTGCGGATTCTTGTG
	Antisense	CGTTTCTTFAAGGCATACTGGTGAG
GAPDH	Sense	ACCACAGTCCATGCCATCAC
	Antisense	TCCACCACCCTGTTGCTGT
PPARγ2 (real-time RT-PCR)	Sense	GATACACTGTCTGCAAACATATCACAA
	Antisense	CCACGGAGCTGATCCCAA
	Probe	AGAGATGCCATTCTGGCCCACCAACTT

2.5. Reverse-transcription polymerase chain reaction (RT-PCR) and quantitative real-time PCR

Total RNA was extracted using TRizol Reagent (Invitrogen, CA, USA) and treated with RNase-Free DNase Set (QIAGEN, Germany) to remove any contaminating genomic DNA. For RT-PCR, cDNA was synthesized using a PrimeScript RT reagent Kit (Takara Bio Inc., Japan), after which RT-PCR was run using ExTaq (Takara Bio Inc.). For quantitative real-time PCR, TaqMan PCR was carried out using a Step One Plus Real-Time PCR System as instructed by the manufacturer (Applied Biosystems, CA, USA). Levels of mRNA were normalized to those of 18S mRNA. The primers used are listed in Table 1.

2.6. Statistical analysis

Data are expressed as means ± S.E.M. Statistical significance was evaluated using ANOVA for comparison among six groups. Values of $P < 0.05$ were considered significant.

3. Results

3.1. Adipogenic differentiation of human iPS and ES cells

Morphological phenotypes, immunoreactivities of Nanog, SSEA-4 and TRA-1-60, and ALP activity of human iPS cells did not differ

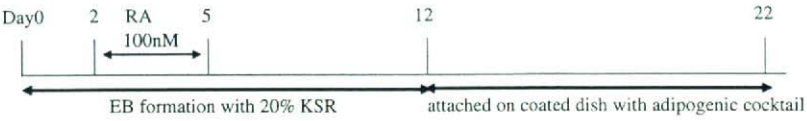

Fig. 1. Schematic diagram of the experimental protocol used for adipocyte differentiation from human ES and human iPS cells. EB: embryoid body. Adipogenic cocktail: 0.5 mM IBMX, 0.25 μM dexamethasone, 1 μg/ml insulin, 0.2 mM indomethacin and 1 μM pioglitazone.

from those of human ES cells (Fig. 2). In order to assess their potential for adipogenic differentiation, the human iPS cells were subjected to adipogenic induction culture. After 12 days of EB formation, EBs derived from human iPS cells were attached to coated dishes to induce differentiation. Several kinds of coating for the dishes, including gelatin, collagen IV and fibronectin were compared, and the efficiency of EB attachment and adipogenic differentiation were the best on dishes coated with a combination of Poly-L-ornithine and fibronectin. On day 15, after 3 days of adipogenic differentiation following the EB formation, differentiated cells containing small cytoplasmic lipid droplets were observed spreading outward from the attached EBs. On day 22, the lipid accumulation was evaluated by staining the cells with Oil Red O.

To evaluate the adipogenic potential of individual iPS cell lines, the percentage of EB outgrowths having adipocyte colonies and the percent area of Oil Red O staining (+) were determined. For each of iPS and ES cell lines tested, 40–60% of EBs formed adipocyte colonies (Table 2). In all of the iPS cell lines, lipid accumulation was similar to that seen in human ES cell lines (Fig. 3), though the B7 line showed stronger lipid accumulation than the other cell lines.

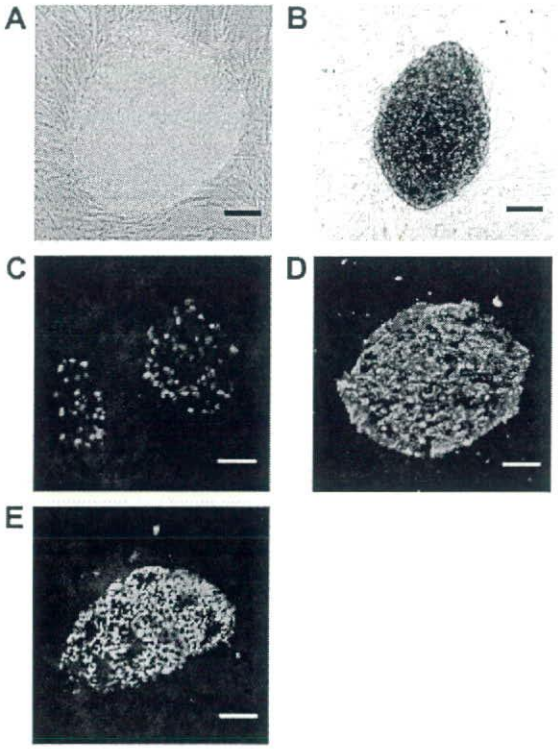

Fig. 2. Morphology of undifferentiated human iPS cells (G4). (A) Phase-contrast photomicrograph of an undifferentiated colony. (B) Alkaline phosphatase activity. (C) Immunofluorescent staining with Nanog. (D) Immunofluorescent staining with SSEA-4. (E) Immunofluorescent staining with TRA1-60. Scale bar = 100 μM.

Table 2
% of EBs with adipocyte colonies.

Cell line	[Number of EBs with adipocytecolonies/total number of EBs]
201B6	54.1% [40/74]
201B7	59.7% [46/77]
253G1	50.0% [35/70]
253G4	56.4% [44/78]
H9	48.8% [39/80]
KhES-1	45.5% [35/77]

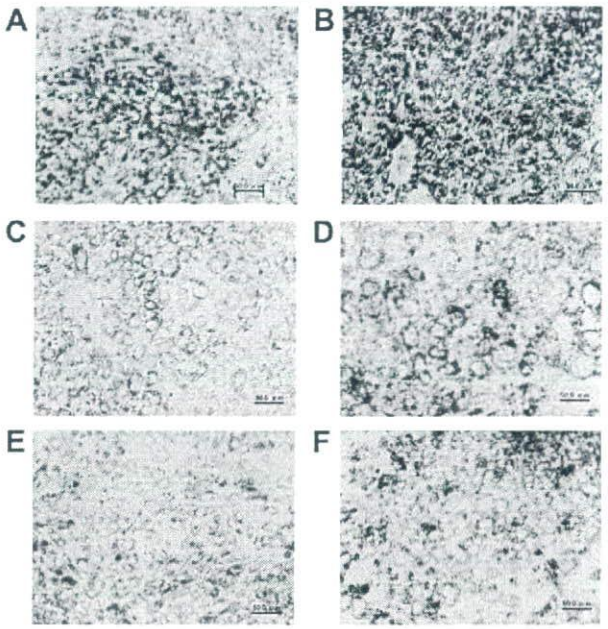

Fig. 3. Oil Red O staining of adipocytes derived from human iPS cells (A–D) and ES cells (E, F) on day 22. B6 (B) B7 (C) G1 (D) G4 (E) H9 (F) KhES-1. Scale bar = 50 μM.

Statistical analysis of the percent area of Oil Red O staining (+) showed no significant differences among the cell lines (Fig. 4).

3.2. Expression of adipogenesis-related molecules

Using RT-PCR, transcription of adipogenic markers was investigated on days 0 and 22 of differentiation (Fig. 5A). Though not detected at day 0, mRNAs encoding the adipogenic transcription factors C/EBPα (CCAAT/enhancer binding protein α) and PPARγ2 (peroxisome proliferator-activated receptor γ2) were detected on day 22. In contrast, expression of Nanog mRNA was strongly suppressed on day 22, as compared with its expression on day 0. Expression of the mature adipocyte markers leptin and aP2 (adipocyte fatty acid binding protein) was also clearly detected on day 22. All of the human iPS cell lines expressed mRNAs encoding adipogenesis-related molecules at levels that were comparable to the levels seen in human ES cell lines (Fig. 5A). In Quantitative real-time PCR analysis, expression of PPARγ2 mRNA differed somewhat among the iPS and ES cell lines. The differences between the B7 line and the two ES cell lines were significant, but other differences were not significant (Fig. 5B).

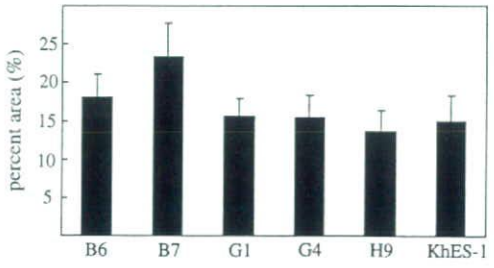

Fig. 4. Percent area of Oil Red O staining. Results are means of six independent experiments. No significant differences were observed among the iPS and ES cell lines.

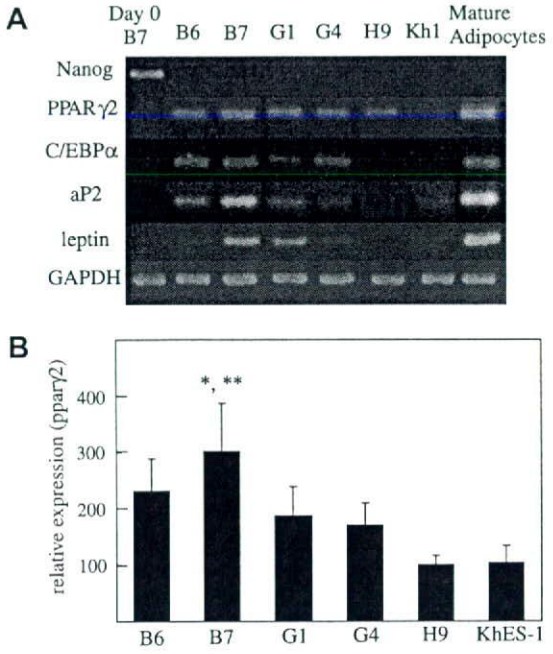

Fig. 5. (A) Transcription of the adipocyte-specific markers PPARγ2, CEBP/α, aP2 and leptin. RNA samples from undifferentiated human iPS cells (B7, day 0) and differentiated stage iPS cells (B6, B7, G1, G4) and human ES cells (H9, KhES-1), as well as mature human adipocytes differentiated from human adipose-derived mesenchymal stem cells (positive control), were analyzed by RT-PCR. Nanog is an undifferentiated human ES cell marker. GAPDH served as an internal standard for RT-PCR. Kh1: KhES-1. Adipose: human mature adipocytes differentiated from human adipose-derived mesenchymal stem cells. (B) Relative levels of PPARγ2 mRNA expression are shown as means ± S.E.M. of 4–6 independent experiments and normalized to those of 18S. The levels are expressed as percentages of the expression in the H9 cell line. $^{*}P < 0.05$ vs. H9. $^{**}P < 0.05$ vs. KhES-1.

4. Discussion

The present study demonstrates that human iPS cells have adipogenic potential comparable to human ES cells. Four human iPS cell lines of two generations were investigated. The B6 and B7 were generated by introducing four transcription factors (Oct3/4, Sox2, Klf4 and c-Myc) into human skin fibroblasts while the G1 and G4 were generated using only three factors (c-Myc was omitted) [9]. After 12 days of embryoid body formation and an additional 10 days of differentiation on Poly-L-ornithine and fibronectin-coated dishes with adipogenic differentiation medium, all human iPS cell lines of both generations exhibited lipid accumulation and transcription of such adipogenesis-related molecules as C/EBPα, PPARγ2, leptin and aP2. We also compared differentiation efficiency between human iPS and ES cells using two lines of human ES cells and found no apparent difference between human iPS and ES cells in properties of adipogenic differentiation including the time course and potential. In terms of lipid accumulation and transcription of adipogenesis-related molecules, human iPS-derived adipocytes appear to reach at least the same level of maturity as those derived from human ES cells. The B7 line tended to show stronger adipogenic potential than the other five iPS lines and the ES cell lines, but the difference in terms of percent area of Oil Red O staining (+) was not significant. The B7 line also showed significantly stronger expression of PPARγ2 than the two ES cell lines tested, but PPARγ2 expression varied among the different iPS cell lines, despite their having the same genetic background. We conclude that the adipogenic potential of iPS cells did not essentially differ from ES cells, though their adipogenic potentials were rather varied in each line.

Despite the prevalence of obesity, systems for research into human adipocyte biology remain underdeveloped, in part because of a lack of available human adipocyte cell lines. There are significant differences between adipocyte development in humans and mice [20]. The established in vitro adipocyte differentiation system using human iPS cells in the present study should make it possible to dissect out the cellular mechanisms underlying human adipocyte differentiation. It should also contribute to the better understanding of adipocyte biology and serve as a basis for advances in research into obesity and adipotoxicity, which has been proposed as the sum of the negative effects associated with obesity [21].

Adipogenesis is largely divided into two phases: the early phase consisting of the lineage commitment of adipocytes from pluripotent stem cells and the late phase consisting of the terminal differentiation of preadipocytes into adipocytes [22]. The molecular mechanism underlying the terminal adipocyte differentiation has been identified through analysis of the differentiation process in immortalized mouse preadipocyte cell lines (e.g., 3T3-L1 and 3T3-F442A cells) [22–24], but the differentiation from pluripotent stem cells during the early stage of adipogenesis must await further clarification. The establishment of adipocyte differentiation system with human iPS cells should facilitate that line of research.

In contrast to human ES cells, iPS cells can be induced from any human being irrespective of their genetic make-up. Consequently, the study of iPS cells should contribute to the identification of new susceptibility genes associated with obesity and metabolic syndrome, and to the clarification of the functions of those genes. The establishment of iPS cell lines from patients with inherited diseases presenting adipocyte abnormality should enable clarification of their pathogenesis. And because they overcome the immunological and ethical problems associated with human ES cells, iPS cell systems should also contribute to the development of novel regenerative therapies for reconstruction of soft tissue defects after tumor resections, extensive deep burns and lipodystrophy. The induced cells obtained with our protocol are not a homogeneous population. Consequently, at this stage human iPS cells may not yet have as much adipogenic potential as adipose-derived stem cells (ADSCs), which are derived from the stromal vascular fraction of human adipose tissue and are thought to be a safe and useful tool in adipose regenerative medicine [25]. About 80% of ADSCs differentiate into adipocytes under suitable conditions [26]. The next issue we plan to address will be the establishment of an improved differentiation protocol that includes a purification process such as cell sorting.

In conclusion, the present study demonstrates that human iPS cells have adipogenic potential that is generally equal to that of human ES cells. The use of iPS cells will contribute to the development of regenerative therapies of adipose tissue for lipodystrophy. This work should also contribute to our understanding of human adipogenesis and to the clarification of the pathogenesis and pathophysiology of obesity and metabolic syndrome, potentially leading to the development of new drug therapies.

Acknowledgement

We thank Yoshie Fukuchi for her technical assistance. This work was supported by the project for realization of regenerative medicine of the Ministry of Education, Culture, Sports, Science and Technology, Japan.

References

[1] Thomson, J.A., Itskovitz-Eldor, J., Shapiro, S.S., Waknitz, M.A., Swiergiel, J.J., Marshall, V.S. and Jones, J.M. (1998) Embryonic stem cell lines derived from human blastocytsts. Science 282, 1145–1147.

[2] Yamashita, J., Itoh, H., Hirashima, M., Ogawa, M., Nishikawa, S., Yurugi, T., Naito, M., Nakao, K., Nishikawa, S., et al. (2000) Flk1-positive cells derived from embryonic stem cells serve as vascular progenitors. Nature 408, 92–96.
[3] Sone, M., Itoh, H., Yamashita, J., Nakao, K., et al. (2003) Different differentiation kinetics of vascular progenitor cells in primate and mouse embryonic stem cells. Circulation 107, 2085–2088.
[4] Sone, M., Itoh, H., Nakao, K., et al. (2007) Pathway for differentiation of human embryonic stem cells to vascular cell components and their potential for vascular regeneration. Arterioscler. Thromb. Vasc. Biol. 27, 2127–2134.
[5] Yamahara, K., Sone, M., Itoh, H., Nakao, K., et al. (2008) Augmentation of Neovascularizaition in hindlimb ischemia by combined transplantation of human embryonic stem cells-derived endothelial and mural cells. PLOS One 3 (2), e1666.
[6] Takahashi, K. and Yamanaka, S. (2006) Induction of pluripotent stem cells from mouse embryonic and adult fibroblast cultures by defined factors. Cell 126, 663–676.
[7] Takahashi, K., Tanabe, K., Ohnuki, M., Narita, M., Ichisaka, T., Tomoda, K. and Yamanaka, S. (2007) Induction of pluripotent stem cells from adult human fibroblasts by defined factors. Cell 131, 861–872.
[8] Yu, J., Vodyanik, M.A., Smuga-Otto, K., Antosiewicz-Bourget, J., Frane, J.L., Tian, S., Nie, J., Jonsdottir, G.A., Ruotti, V., Stewart, R., Slukvin II and Thomson, J.A. (2007) Induced pluripotent stem cell lines derived from human somatic cells. Science 318, 1917–1920.
[9] Nakagawa, M., Koyanagi, M., Tanabe, K., Takahashi, K., Ichisaka, T., Aoi, T., Okita, K., Mochiduki, Y., Takizawa, N. and Yamanaka, S. (2008) Generation of induced pluripotent stem cells without Myc from mouse and human fibroblasts. Nat. Biotechnol. 26, 101–106.
[10] Ebihara, K., Kusakabe, T., Masuzaki, H., Kobayashi, N., Tanaka, T., Chusho, H., Miyanaga, F., Miyazawa, T., Hayashi, T., Hosoda, K., Ogawa, Y. and Nakao, K. (2004) Gene and phenotype analysis of congenital generalized lipodystrophy in Japanese: a novel homozygous nonsense mutation in seipin gene. J. Clin. Endocrinol. Metab. 89 (5), 2360–2364.
[11] Ebihara, K., Masuzaki, H. and Nakao, K. (2004) Long-term leptin-replacement therapy for lipoatrophic diabetes. New Engl. J. Med. 351 (6), 615–616.
[12] Ebihara, K., Kusakabe, T., Hirata, M., Masuzaki, H., Miyanaga, F., Kobayashi, N., Tanaka, T., Chusho, H., Miyazawa, T., Hayashi, T., Hosoda, K., Ogawa, Y., DePaoli, AM., Fukushima, M. and Nakao, K. (2007) Efficacy and safety of leptin-replacement therapy and possible mechanisms of leptin actions in patients with generalized lipodystrophy. J. Clin. Endocrinol. Metab. 92 (2), 532–541.
[13] Ebihara, K., Ogawa, Y., Masuzaki, H., Shintani, M., Miyanaga, F., Aizawa-Abe, M., Hayashi, T., Hosoda, K., Inoue, G., Yoshimasa, Y., Gavrilova, O., Reitman, ML. and Nakao, K. (2001) Transgenic overexpression of leptin rescues insulin resistance and diabetes in a mouse model of lipoatrophic diabetes. Diabetes 50 (6), 1440–1448.
[14] Fujioka, T., Yasuchika, K., Nakamura, Y., Nakatsuji, N. and Suemori, H. (2004) A simple and efficient cryopreservation method for primate embryonic stem cells. Int. J. Dev. Biol. 48, 1149–1154.
[15] Dani, C., Smith, A.G., Ailhaud, G., et al. (1997) Differentiation of embryonic stem cells into adipocytes in vitro. J. Cell. Sci. 110, 1279–1285.
[16] Xiong, C., Xie, C.Q., Chen, Y.E., et al. (2005) Derivation of adipocytes from human embryonic stem cells. Stem Cells Dev. 14, 671–675.
[17] van Harmelen, V., Astrom, G., Ryden, M., et al. (2007) Differential lipolytic regulation in human embryonic stem cell-derived adipocytes. Obesity 15, 846–852.
[18] Barberi, T., Willis, L.M., Socci, N.D. and Studer, L. (2005) Derivation of multipotent mesenchymal precursors from human embryonic stem cells. PLoS Med. 2, e161.
[19] Olivier, E.N., Rybicki, A.C. and Bouhassira, E.E. (2006) Differentiation of human embryonic stem cells into bipotent mesenchymal stem cells. Stem cells 24, 1914–1922.
[20] Arner, P. (2005) Resistin: yet another adipokine tells us that men are not mice. Diabetologia 48, 2203–2205.
[21] Nakao, K. (2009) Adiposcience and adipotoxicity. Nat. Clin. Pract. Endocrinol. Metab. 5 (2), 63.
[22] Rosen, E.D. and Spiegelman, B.M. (2000) Molecular regulation of adipogenesis. Annu. Rev. Cell. Dev. Biol. 16, 145–171.
[23] Bernlohr, D.A., Bolanowski, M.A., Kelly Jr., T.J. and Lane, M.D. (1985) Evidence for an increase in transcription of specific mRNAs during differentiation of 3T3-L1 preadipocytes. J. Biol. Chem. 260, 5563–5567.
[24] Flier, J.S. (2004) Obesity wars: molecular progress confronts an expanding epidemic. Cell 116, 337–350.
[25] Zuk, P.A., Zhu, M., Mizuno, H., Huang, J., Futrell, J.W., et al. (2001) Multilineage cells from human adipose tissue: Implications for cell-based therapies. Tissue Eng. 7, 211–228.
[26] Zhu, Y., Liu, T., Song, K., Fan, X., Ma, X. and Cui, Z. (2008) Adipose-derived stem cell: a better stem cell than BMSC. Cell Biochem. Funct. 26, 664–675.

0888-8809/08/$15.00/0
Printed in U.S.A.

Molecular Endocrinology 22(9):2176–2189

doi: 10.1210/me.2008-0023

Dysregulation of Adipose Glutathione Peroxidase 3 in Obesity Contributes to Local and Systemic Oxidative Stress

Yun Sok Lee, A Young Kim, Jin Woo Choi, Min Kim, Shintaro Yasue, Hee Jung Son, Hiroaki Masuzaki, Kyong Soo Park, and Jae Bum Kim

Institute of Molecular Biology and Genetics (Y.S.L., A.Y.K., J.W.C., J.B.K.) and Department of Biological Sciences, Research Center for Functional Cellulomics (Y.S.L., A.Y.K., J.W.C., J.B.K.), Seoul National University, Seoul 151-742, Korea; Department of Internal Medicine (M.K., K.S.P.), Seoul National University College of Medicine, Seoul 110-744, Korea; Department of Medicine and Clinical Science (S.Y., H.M.), Kyoto University Graduate School of Medicine, Kyoto 606-8507, Japan; and Samsung Medical Center (H.J.S.), Seoul 135-230, Korea

Glutathione peroxidase 3 (GPx3) accounts for the major antioxidant activity in the plasma. Here, we demonstrate that down-regulation of GPx3 in the plasma of obese subjects is associated with adipose GPx3 dysregulation, resulting from the increase of inflammatory signals and oxidative stress. Although GPx3 was abundantly expressed in kidney, lung, and adipose tissue, we observed that GPx3 expression was reduced selectively in the adipose tissue of several obese animal models as decreasing plasma GPx3 level. Adipose GPx3 expression was greatly suppressed by prooxidative conditions such as high levels of TNFα and hypoxia. In contrast, the antioxidant *N*-acetyl cysteine and the antidiabetic drug rosiglitazone increased adipose GPx3 expression in obese and diabetic *db/db* mice. Moreover, GPx3 overexpression in adipocytes improved high glucose-induced insulin resistance and attenuated inflammatory gene expression whereas GPx3 neutralization in adipocytes promoted expression of proinflammatory genes. Taken together, these data suggest that suppression of GPx3 expression in the adipose tissue of obese subjects might constitute a vicious cycle to expand local reactive oxygen species accumulation in adipose tissue potentially into systemic oxidative stress and obesity-related metabolic complications. (*Molecular Endocrinology* 22: 2176–2189, 2008)

ADIPOSE TISSUE contributes to maintaining the energy homeostasis of the whole body not only by buffering lipid metabolites but also by secreting several adipocytokines in response to the inputs of the central nervous system and periphery (1). In obesity, however, adipose tissue fails to accommodate fatty acids effectively according to the changing metabolic requirements, resulting in excessive accumulation of lipid metabolites in peripheral tissues, including the liver and muscle tissues, along with adipocytokine dysregulation (2). The abnormal regulation of adipocytokines occurring in obesity affects the functions of other tissues, including the liver, muscle, central nervous system, and vasculatures, thus increasing the risks for metabolic complications. Therefore, it appears that examining the molecular regulatory mechanisms for adipocytokines in obesity is crucial for understanding metabolic disorders and for developing effective therapeutic interventions for obesity and its related complications.

One of the main clinical manifestations of obesity is increased systemic oxidative stress (3–5). Oxidative stress has been implicated in several forms of tissue damage and leads to pathological conditions such as irradiation damage and ischemia reperfusion injury, as well as neurodegenerative diseases (6, 7). However, accumulating evidence indicates that increased oxidative stress is also strongly associated with metabolic disorders, including atherosclerosis, thrombosis, liver steatosis, and diabetes mellitus, which are often observed in morbid obesity (8–11). Reactive oxygen species (ROS) can rapidly inactivate vascular nitrogen oxide (NO), a major vasorelaxant and inhibitor of platelet function, and can increase the risks for atherosclerosis and stroke. Moreover, posttranslational modifications of fibrinogen by ROS and NO-derived oxidants enhance fibrinogen activity, thus accelerating clot formation and thrombosis (12, 13). In addition, oxidative stress impairs insulin secretion by the pancreatic

First Published Online June 18, 2008

Abbreviations: BAT, Brown adipose tissue; CAT, catalase; ChIP, chromatin immunoprecipitation; f, forward; GPx3, glutathione peroxidase 3; iNOS, inducible nitric oxide synthase; LPO, lipid peroxidation; LPS, lipopolysaccharide; NAC, *N*-acetyl cysteine; NADPH, reduced nicotinamide adenine dinucleotide phosphate; PPAR, peroxisomal proliferator-activated receptor; PPRE, PPAR response element; r, reverse; ROS, reactive oxygen species; RXR, retinoid X receptor; SVC, stromal vascular cell; TBARS, thiobarbituric acid-reactive substances; TZD, thiazolidinedione; WAT, white adipose tissue.

***Molecular Endocrinology* is published monthly by The Endocrine Society (http://www.endo-society.org), the foremost professional society serving the endocrine community.**

β-cells (14) as well as glucose transport into the muscle (15) and adipose tissue (16).

Recently, it has been shown that ROS generation is selectively increased in the fat tissues of obese mice, resulting in insulin resistance and dysregulation of adipocytokine gene expression (5). Interestingly, several insulin resistance-inducing factors such as TNFα and dexamethasone, as well as free fatty acids and high glucose levels, potently stimulate ROS production in adipocytes (5, 17, 18). On the other hand, antioxidant molecules such as *N*-acetyl cysteine (NAC), manganese (III) tetrakis (4-benzoic acid) porphyrin, and apocynin not only reverse TNFα-induced dysregulation of adipocytokine gene expression but also ameliorate insulin resistance, hyperlipidemia, and liver steatosis in obese animals, without altering the body weight (5, 17). Thus, it appears that increased systemic oxidative stress stemming from the expansion of adipose tissue during developing obesity may play a role in mediating obesity-related metabolic complications.

The cellular redox potential is maintained by a balanced regulation of prooxidative and antioxidative enzymes. The catalytic triad of superoxide dismutase, catalase (CAT), and glutathione peroxidase (GPx) is an antioxidant system for removing superoxide anions and is well conserved from prokaryotes to eukaryotes (12). Superoxide dismutase converts superoxide anions to H_2O_2, which is further catalyzed by GPx and CAT into a harmless product, H_2O. CAT recognizes only H_2O_2 as its substrate and functions with very low affinity (19). Thus, it mainly functions only at H_2O_2 levels above the physiological level; these conditions may arise during oxidative burst in response to stress. On the other hand, GPx metabolizes peroxidized organic molecules as well as H_2O_2, recycles some of the molecules attacked by H_2O_2 with a relatively high affinity, and catalyzes these molecules even at the normal physiological concentrations (20). Therefore, GPx activity is considered to represent the initial protective response required for adjusting the H_2O_2 concentration under normal physiological conditions as well as after oxidative insult.

To date, seven isoforms of GPx proteins have been identified in mice (21). Of these, only GPx3 is found in the plasma and accounts for a major part of the plasma GPx activity (21). A large amount of GPx3 is synthesized in and secreted from the kidneys and lungs; it maintains the bioavailability of vascular NO and scavenges H_2O_2 and peroxidized organic molecules in the plasma to reduce systemic oxidative stress (22, 23).

In this study, we demonstrated that GPx3 was highly expressed in the adipose tissue, and its expression was reduced in both sera and fat tissues of obese subjects. Because GPx3 was reduced selectively in the fat tissues of obese mice, we propose that elevated systemic oxidative stress in obesity is associated with reduced circulating GPx3 expression, probably by diminished adipose GPx3 expression.

RESULTS

Systemic Oxidative Stress in Obesity Is Associated with Reduced Circulating GPx3 Expression

Recently, it has been reported that a systemic increase in oxidative stress is often observed in obese subjects and is regarded to be directly involved in increasing incidence of obesity-related metabolic complications including diabetes mellitus and cardiovascular diseases (3–5). Consistent with these reports, we observed that obese and diabetic *db/db* mice exhibited increased plasma ROS and oxidative damages, which were assessed in terms of thiobarbituric acid-reactive substances (TBARS) concentration (Fig. 1, A and B). While analyzing protein expression profile in the plasma of normal and obese mice, we found that the circulating GPx3 level was greatly decreased in the obese subjects (Fig. 1C). Concurrently, we observed that the total GPx activity in the plasma was reduced in the obese mice (Fig. 1D). Similar to the data obtained from the obese animal models, the plasma levels of the GPx3 protein and the total plasma GPx activity were substantially diminished even in obese human subjects (Fig. 1, E and F). These results suggest that increased oxidative stress in obesity appears to be linked with reduced circulating GPx3 expression.

GPx3 Is Abundantly Expressed in Adipose Tissue as Well as Kidney and Lung

To examine tissue distribution of the GPx3, we performed Northern blot analyses with mouse tissues. Previously, it has been shown that GPx3 is abundantly expressed in kidney, lung, and fat tissue in humans (24). Consistently, we observed that GPx3 mRNA was highly expressed in the kidney, lung, and white adipose tissue (WAT) of B6 mice (Fig. 2A). Moreover, GPx3 was highly expressed in brown adipose tissue (BAT) (Fig. 2A). In addition, GPx3 expression in the WAT was remarkably reduced in diet-induced obese mice than in the control mice (Fig. 2A).

Next, we determined relative expression of GPx3 in adipocytes and stromal vascular cells (SVCs) isolated from the adipose tissue. Recently, it was reported that GPx3 is induced during adipogenesis of human and bovine preadipocytes (25, 26). In accordance with this report, GPx3 was more abundantly expressed in adipocytes than in SVCs of B6 mouse adipose tissue (Fig. 2B). Moreover, its mRNA expression was elevated during adipocyte differentiation of 3T3-L1 (Fig. 2C). We also examined the expression of adiponection mRNA as a control for adipocyte marker gene (27). However, the GPx3 mRNA level was considerably lower (<250-fold less) in the 3T3-L1 adipocytes than in the mouse primary adipocytes, as frequently observed in other cell lines derived from the tissues abundantly expressing GPx3 (28).

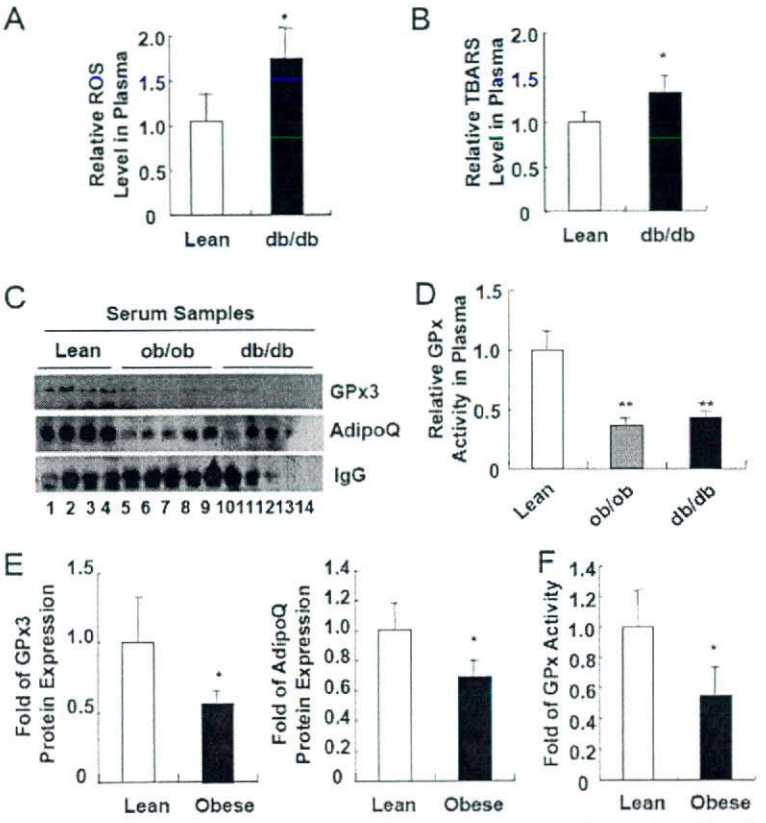

Fig. 1. Systemic Increase in Oxidative Stress in Obese Subjects Is Associated with Decreasing Circulating GPx3 Expression

A, ROS concentration in the serum samples obtained from lean and obese *db/db* mice. B, Systemic oxidative damage as reflected by the TBARS concentrations in the serum samples from lean and obese *db/db* mice. The values represent the means ± SEM (n = 4 or 8). C, Western blot analyses of GPx3 protein expression in the serum samples of lean, *ob/ob*, and *db/db* mice. D, GPx activity assays on the serum samples from lean and obese mice. E and F, GPx3 protein expression (E) and GPx activity (F) are reduced in the serum of obese human subjects. Lean, body mass index <25; obese, body mass index >30. *Error bars* indicate the SEM (n = 3 or 4). *, $P < 0.05$; **, $P < 0.01$. AdipoQ, Adiponectin.

GPx3 Expression Is Reduced in the Adipose Tissue, But Not Kidney, of Obese Mice

Because GPx3 mRNA was expressed most abundantly in kidney, we decided to determine whether the diminished circulating GPx3 level in obese subjects is associated with GPx3 expression in the kidneys. When we analyzed GPx3 expression, both mRNA and protein levels of GPx3 were not altered or even slightly increased in the kidneys of *ob/ob* and *db/db* obese mice (Fig. 3A) (see supplemental Figs. 1 and 2 published as supplemental data on The Endocrine Society's Journals Online web site at http://mend.endojournals.org data). In contrast, GPx3 mRNA was significantly reduced in the WAT of obese animal models including *ob/ob* and *db/db* mice, as compared with that in lean mice (Fig. 3B); this result is consistent with the previous report that GPx3 is suppressed in the adipose tissue of obese fatty OLETF rats (29). Further, a similar reduction in the GPx3 expression was selectively observed in several adipose tissues of obese mice (supplemental Fig. 2). Furthermore, reduced GPx3 expression was mainly observed in the adipocytes but not in the SVCs isolated from the WAT of *db/db* mice (Fig. 3C) (supplemental Fig. 3). Notably, TNFα was induced in the WAT of *ob/ob* and *db/db* mice (Fig. 3B) as expected (30). Moreover, the GPx3 protein level and total GPx activity in the WAT of obese *ob/ob* and *db/db* mice were significantly diminished (Fig. 3, D and E). Concurrent with these findings, the levels of total ROS and TBARS found to be elevated in the WAT of *db/db* mice (Fig. 3, F and G). Together, it is likely that reduced plasma GPx3 levels observed in obese subjects is presumably due to reduced GPx3 expression in the fat tissues rather than in the kidneys (Figs. 1–3).

Adipose GPx3 Expression Is Suppressed by TNFα, Lipopolysaccharide (LPS), and Hypoxia, Whereas It Is Stimulated by the Antioxidant NAC

It is well established that obesity is closely associated with ROS accumulation and with increased proinflammatory gene expression in adipose tissue (5, 30). Functioning as a key proinflammatory cytokine, TNFα expression is elevated in the fat tissues of obese mice, and it stimulates the expression of prooxidative genes

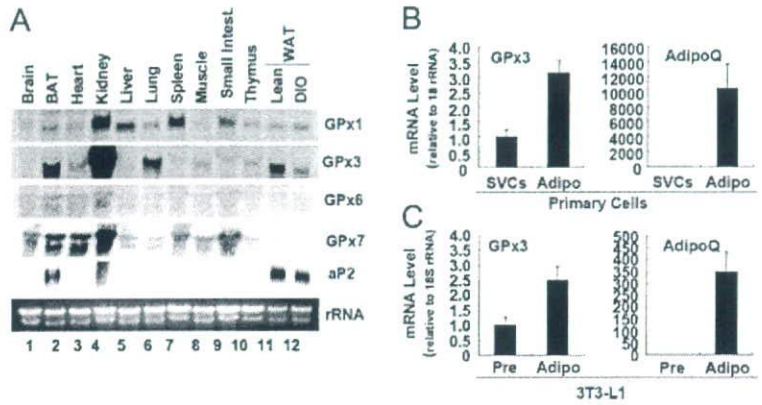

Fig. 2. GPx3 Is Abundantly Expressed in Adipose Tissue

A, Total RNA was isolated from several tissues of lean C57BL6 mice and was subjected to Northern blot analyses. DIO, Diet-induced obese. B, GPx3 mRNA expression in the two fractions—SVCs and adipocytes (Adipo)—obtained by collagenase digestion of WAT. Total RNA isolated from each fraction was analyzed by quantitative real-time RT-PCR. Adiponectin (AdipoQ) was used as a maker gene of adipocytes. C, GPx3 mRNA expression in the preadipocytes (Pre) and adipocytes (Adipo) of 3T3-L1 was analyzed by quantitative real-time RT-PCR. *Error bars* indicate the SEM (n = 3).

such as inducible nitric oxide synthase (iNOS) and nicotinamide adenine dinucleotide phosphate (NADPH) oxidase (30). To determine whether this augmented expression of TNFα is related to the reduced adipose GPx3 expression observed in obese mice, we treated 3T3-L1 adipocytes as well as mouse epididymal fat tissue with TNFα and analyzed their GPx3 mRNA expression. As previously reported (31, 32), TNFα induced inflammatory genes, including TNFα, SAA3, and iNOS, whereas it decreased the peroxisomal proliferator-activated receptor (PPAR)γ and adiponectin mRNA levels (Fig. 4, A and B). Interestingly, TNFα significantly decreased the GPx3 expression in both 3T3-L1 adipocytes and epididymal fat tissue (Fig. 4, A and B; and see supplemental Fig. 4).

To directly ascertain whether inflammatory signals affect the adipose GPx3 expression *in vivo*, lean mice were treated with LPS, and the GPx3 mRNA expression levels and total GPx activities in fat tissues were measured. As shown in Fig. 4, C and D, both GPx3 expression and GPx activity were repressed in the adipose tissue by LPS-induced systemic inflammation, whereas the level of kidney GPx3 mRNA was enhanced by LPS (Fig. 4E). These results imply that increased inflammatory signals present in obesity could selectively down-regulate adipose GPx3 expression.

Hypoxic conditions stimulate ROS generation in several cell types and induce inflammatory gene expression (33). Recent reports have demonstrated the adipose tissue of obese mice to be hypoxic (34, 35), and hypoxia interferes with adipocyte differentiation as well as adipocytokine expression (36–38). To examine the effects of hypoxia on adipose GPx3 expression, 3T3-L1 adipocytes were treated with $CoCl_2$, a well-known hypoxia mimetic (37, 39–41). As expected, treatment of $CoCl_2$ reduced the expression of PPARγ and adiponectin, whereas it stimulated vascular endothelial growth factor expression (36) (Fig. 4F). Simultaneously, $CoCl_2$ markedly suppressed GPx3 expression (Fig. 4F); this implies that hypoxia might also be a possible factor for the reduced adipose GPx3 expression observed in obese animals.

To clarify whether the decreased adipose GPx3 expression occurring in obesity may be due to oxidative stress with chronic inflammation and/or hypoxia, we administered a potent antioxidant chemical, NAC, to obese *db/db* mice, and we examined the GPx3 expression in the fat tissues. In accordance with the *in vitro* and *in vivo* data described above, NAC treatment enhanced GPx3 expression but reduced iNOS expression in the fat tissues of *db/db* mice (Fig. 4G). In contrast, GPx3 expression in the kidneys was reduced by NAC treatment in *db/db* mice (Fig. 4H), implying that GPx3 may be regulated by distinct mechanisms in adipose tissue and kidney in response to oxidative stress. Taken together, these *in vitro*, *ex vivo*, and *in vivo* data suggest that the reduced adipose GPx3 expression observed in obese mice would be tightly regulated by oxidative insults as well as inflammatory signals in an adipose tissue-specific manner.

Rosiglitazone and PPARγ Stimulate GPx3 Expression

Functioning as a master transcription factor for adipogenesis, PPARγ is involved in regulating the expression of several adipocytokine genes, including leptin, resistin, and adiponectin (42). PPARγ activation by its ligand thiazolidinediones (TZDs) improves insulin sensitivity and protects cells from oxidative stress-induced apoptosis (43–47). Because GPx3 was abundantly expressed in the WAT and BAT, we investigated the effects of PPARγ activation on adipose GPx3 expression. After treating 3T3-L1 adipocytes with rosiglitazone, the GPx3 mRNA level was dramatically elevated (Fig. 5A). Moreover, the administration of rosiglitazone

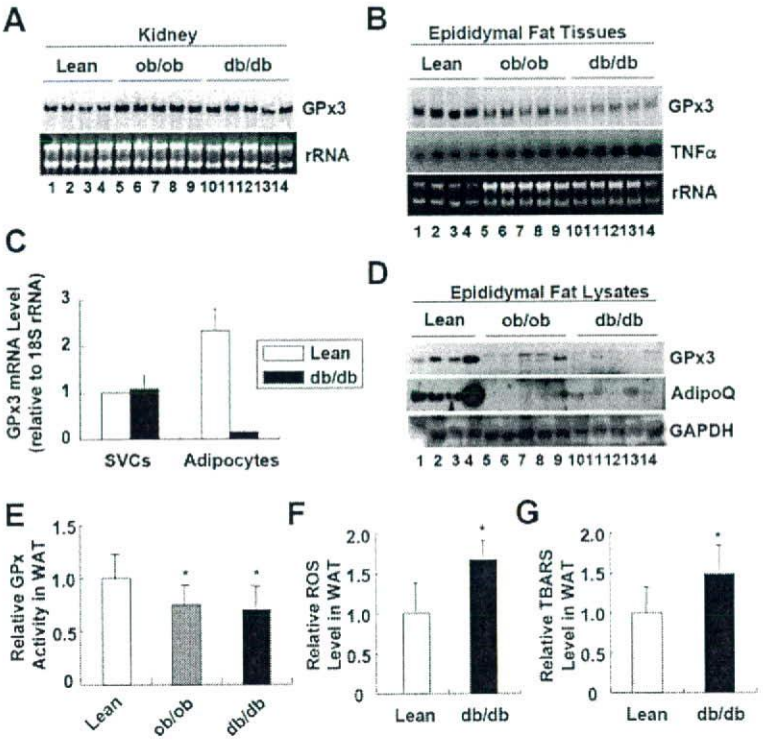

Fig. 3. GPx3 Is Reduced in the Fat Tissue, but not in the Kidney of Obese Mice

A, Northern blot analysis of GPx3 mRNA expression in the kidneys of lean, *ob/ob*, and *db/db* mice. B, Northern blot analysis of GPx3 mRNA expression in the fat tissues of lean, *ob/ob*, and *db/db* mice. C, GPx3 mRNA expression was analyzed in the two fractions (SVCs and adipocytes) obtained by collagenase digestion of adipose tissue from lean and *db/db* mice. Total RNA isolated from each fraction was analyzed by quantitative real-time RT-PCR. D, Western blot analyses of GPx3 protein expression in the fat tissues obtained from lean, *ob/ob*, and *db/db* mice. E, GPx activity assays on the total lysates of epididymal fat tissues from lean and obese mice. F, ROS concentration in the total lysates of fat tissue from lean and obese *db/db* mice. G, Systemic oxidative damage as reflected by the TBARS concentrations in the total lysates of fat tissues obtained from lean and obese *db/db* mice. The values represent the means ± SEM (n = 4 or 8). *, $P < 0.05$ for lean mice *vs.* *ob/ob* or *db/db* mice, indicating a significant difference between the groups. AdipoQ, Adiponectin.

to *db/db* mice restored the GPx3 expression in the fat tissues up to the level observed in lean mice (Fig. 5B) and abated oxidative stress, as reflected by the TBARS levels (Fig. 5C). However, GPx3 expression in kidney was not altered by rosiglitazone treatment (supplemental Fig. 5). To assess whether PPARγ is involved in the expression of adipose GPx3, we analyzed the mouse GPx3 promoter and found, at least, three putative PPAR response element (PPRE) motifs localized approximately at −1.4 kb (PPRE1), −2.4 kb (PPRE2), and −3.1 kb (PPRE3) away from the transcription start site (Fig. 5D). Next, we performed gel shift assays with ARE7 containing an endogenous PPRE from aP2 gene (48). As shown in Fig. 5E, all the three putative PPRE motifs from mouse GPx3 promoter competed with ARE7 probe, suggesting that the three PPREs might be potential binding sites for PPARγ/retinoid X receptor (RXR)α *in vitro*. For further analysis of the PPREs in mouse GPx3 promoter, PPARγ binding activity was determined with chromatin immunoprecipitation (ChIP) assays in adipocytes. As shown in Fig. 5F, substantial binding of PPARγ was detected only around PPRE3, but not PPRE1 and PPRE2, in adipocytes in the presence of rosiglitazone. These results suggest that PPARγ could stimulate GPx3 expression through binding to the mouse GPx3 promoter, and that the activation of PPARγ with TZD could reduce systemic oxidative stress, at least partially, by up-regulating the GPx3 expression in the fat tissues.

GPx3 Overexpression in Adipocytes Ameliorates High-Glucose-Induced Inflammatory Gene Expression and ROS Accumulation, Whereas GPx3 Neutralization Enhances Inflammatory Gene Expression

To gain further insights into the roles of GPx3 in adipocytes, we adenovirally overexpressed GPx3 in 3T3-L1 adipocytes and incubated the cells with sodium selenite because GPx3 is a selenocystein-containing protein (10). Analysis of the inflammatory gene expression profiles in the presence or absence of a hyperglycemic challenge revealed that GPx3 overexpression in 3T3-L1 adipocytes significantly repressed the high-glucose-induced expression of proinflammatory genes such as SAA3, resis-

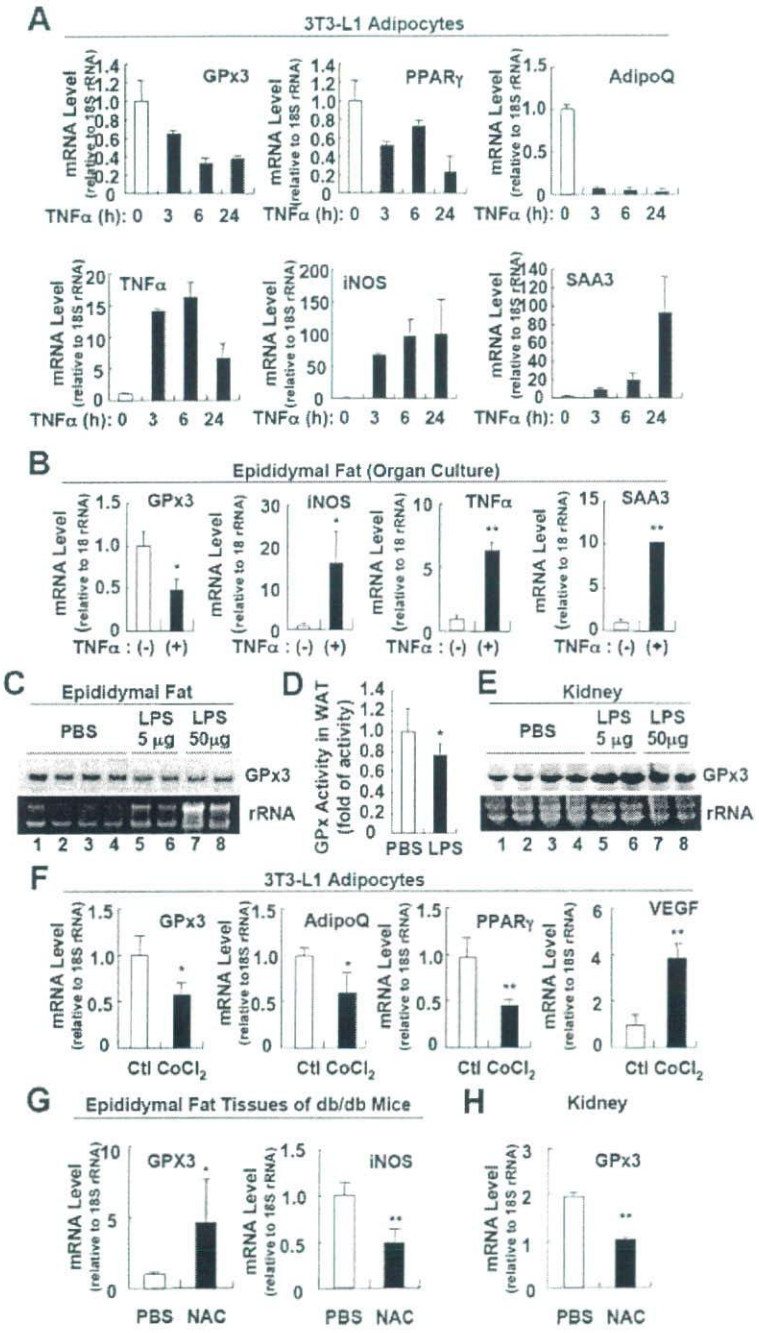

Fig. 4. Adipose GPx3 Expression Is Suppressed by TNFα, LPS, and Hypoxia and Is Stimulated by the Antioxidant NAC

A and B, Adipose GPx3 is suppressed by TNFα. 3T3-L1 adipocytes (A) or epididymal fat tissue (B) was incubated with TNFα (10 ng/ml), and the expression of each gene was analyzed by quantitative real-time RT-PCR. +, TNFα treatment for 8 h. *Error bars* indicate the SEM (n = 2). C, Northern blot analysis of GPx3 mRNA expression in fat tissues obtained from vehicle- and LPS-treated lean mice. LPS was administered to lean C57/BL6 mice as an ip injection for 24 h (5 μg) or 4 h (50 μg). D, GPx activity assays for total lysates of fat tissues obtained from control and LPS-treated (5 μg, 24 h) mice. *Error bars* indicate the SEM (n = 4). E, Northern blot analysis of GPx3 mRNA expression in kidney from vehicle- and LPS-treated lean mice. LPS was administered to lean C57/BL6 mice as an ip injection for 24 h (5 μg) or 4 h (50 μg). F, GPx3 expression in adipocytes is repressed by hypoxia. 3T3-L1 adipocytes were incubated with $CoCl_2$ (100 μM) for 24 h. The expression of each gene was analyzed by quantitative real-time RT-PCR. *Error bars* indicate the SEM (n = 2). G and H, Differential regulation of GPx3 expression in the adipose tissue (G) and the kidneys (H) by the antioxidant NAC. *db/db* mice were ip injected with NAC for 1 wk. Expression of each mRNA was analyzed by quantitative real-time RT-PCR. *Error bars* indicate the SEM (n = 3). *, $P < 0.05$; **, $P < 0.01$ for vehicle- *vs.* drug-treated group, indicating a significant difference between the groups. AdipoQ, Adiponectin; Ctl, control.

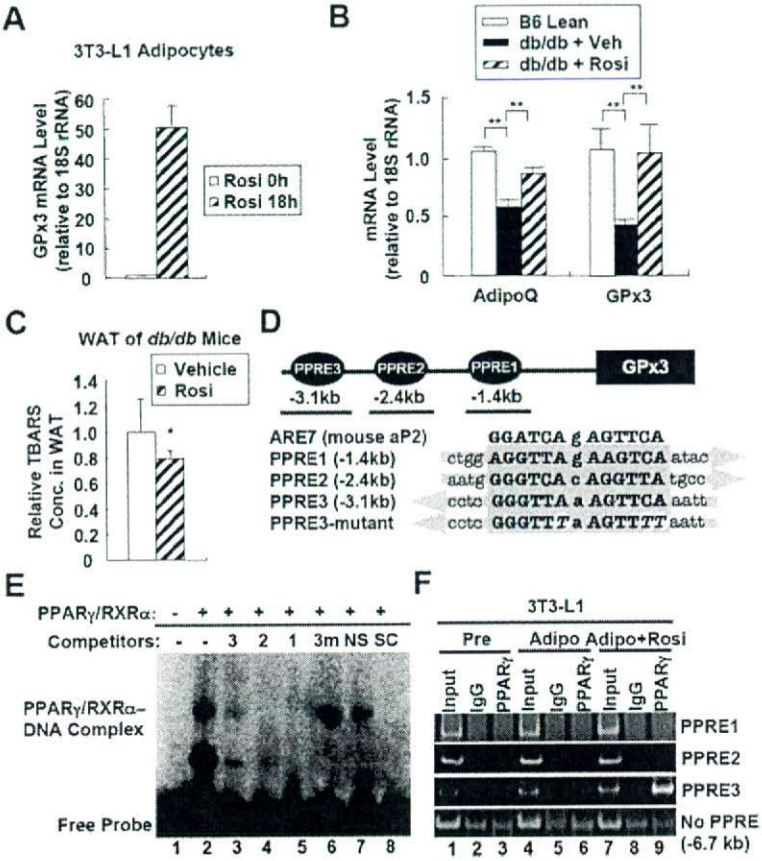

Fig. 5. GPx3 Is Regulated by Rosiglitazone and PPARγ

A, GPx3 expression in adipocytes is induced by rosiglitazone. 3T3-L1 adipocytes were incubated with or without rosiglitazone for 18 h. The mRNA levels were analyzed by quantitative real-time RT-PCR. *Error bars* indicate the SEM (n = 2). B, Adipose GPx3 expression is stimulated by rosiglitazone in *db/db* mice. *db/db* Mice were administered an oral gavage of rosiglitazone (5 mg/kg) for 10 d. Total RNA was prepared from the epididymal fat tissues and was subjected to real-time RT-PCR analysis. *Error bars* indicate the SEM (n = 4). **, $P < 0.01$. C, Systemic oxidative damage as reflected by the TBARS concentrations in the serum samples obtained from normal and *db/db* mice. The values represent the means ± SEM (n = 4). *, $P < 0.05$. D, Schematic presentation of putative PPRE motifs in the mouse GPx3 promoter region. E, Gel shift assays were performed with ^{32}P-labeled ARE7 oligonucleotide containing an endogenous PPRE on the enhancer region of mouse aP2 gene as a probe and *in vitro* translated PPARγ and RXRα proteins. The specific probe-PPARγ/RXRα complex was abolished by addition of 100-fold molar excess of unlabeled ARE7 (lane 8) and the three putative PPRE motifs (lanes 3–5), but not E-box (lane 7) and PPRE3-mutant. In competitors, 3, PPRE3; 2, PPRE2; 1, PPRE1; 3m, PPRE3 mutant; NS, nonspecific competitor (E-box); SC, specific competitor (ARE7). F, ChIP analysis of GPx3 promoter. 3T3-L1 preadipocytes or fully differentiated adipocytes were incubated with or without rosiglitazone (10 μM) for 48 h. For each experiment, 0.5% of input was used. IgG, Purified nonspecifc IgG; PPARγ, anti-PPARγ antibody; AdipoQ, adiponectin; Rosi, rosiglitazone; Veh, vehicle.

tin, and CCR2 (18, 49) (Fig. 6). Additionally, it suppressed the expression of the p47 and p67 subunits of the NADPH-oxidase complex (Fig. 6), which are regulated by nuclear factor-κB and TNFα (50). More interestingly, ROS released from the adipocytes into the medium were reduced by GPx3 overexpression under high glucose conditions (Fig. 7A). Because ROS has been reported to trigger insulin resistance in adipocytes (17, 18), we examined the effects of GPx3 overexpression on high-glucose-induced insulin resistance. Incubation of 3T3-L1 adipocytes in high-glucose media substantially reduced the insulin-stimulated glucose uptake (by ~33%) (18), whereas GPx3 overexpression in 3T3-L1 adipocytes restored the insulin-stimulated glucose uptake under the same conditions (Fig. 7, B and C).

To confirm the effects of adipose GPx3 on inflammatory gene expression, we tried to perform loss-of-function experiments in adipocytes. Because 3T3-L1 adipocytes expressed extremely low levels of GPx3 compared with primary adipocytes, we failed to obtain substantial knockdown of GPx3 expression via siRNA. Alternatively, we adopted antibody-assisted neutralization with primary mouse adipocytes. As illustrated in Fig. 8A, treatment of GPx3-specific antibodies to neutralize secreted GPx3 from adipocytes promoted the expression of several inflammatory genes. Of in-

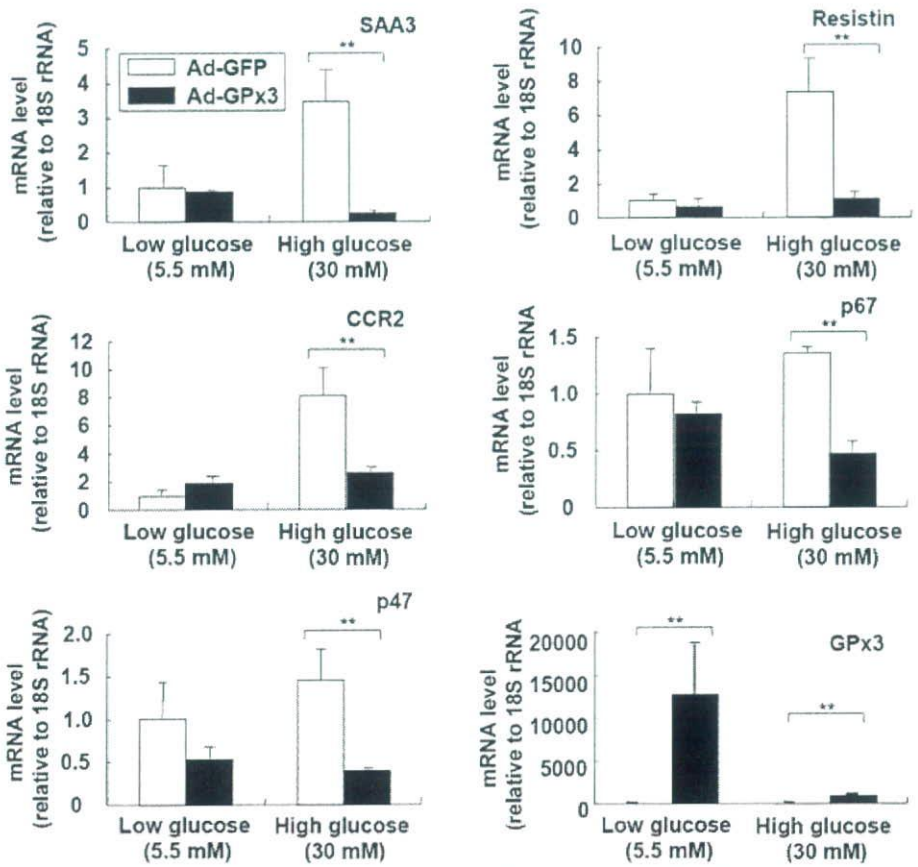

Fig. 6. Adenoviral Overexpression of GPx3 in Adipocytes Reduces Proinflammatory Gene Expression in Adipocytes

3T3-L1 adipocytes were infected with a green fluorescent protein (GFP)- or GPx3-expressing adenovirus (multiplicity of infection = 50). Two days after infection (>80% of cells were GFP positive), the cells were incubated with low (5.5 mM)- or high (25 mM)-glucose DMEM for additional 24 h. The medium was supplemented with sodium selenite (0.1 μM) throughout the experiments. The mRNA levels of proinflammatory genes were analyzed by quantitative real-time RT-PCR. SEM are indicated by the *error bars* (n = 2). **, $P < 0.01$. Ad-GFP, Adenoviral GFP.

terest, the level of GPx3 protein in the adipocyte-conditioned media was comparable to that observed in plasma of lean B6 mice, suggesting that GPx3 concentration might be enough to mediate antioxidative properties (Fig. 8B). Taken together, these results strongly indicate that GPx3 overexpression in adipocytes would alleviate the proinflammatory gene expression and oxidative burst induced by hyperglycemia and ameliorate high-glucose-induced insulin resistance.

DISCUSSION

Accumulating evidence indicates that expanding stressful conditions in the adipose tissue of obesity, including hypoxia and macrophage infiltration, could induce local inflammation and ROS accumulation to affect dysregulation of adipocytokine genes and systemic oxidative stress, resulting in metabolic abnormalities. Recently, it has been also shown that oxidative stress increases selectively in the adipose tissue of obesity, which confers systemic oxidative stress to raise risks for obesity-related metabolic complications (5). As plausible candidates fetching oxidative stress in the adipose tissue of obesity, we and others reported that the activities of the NADPH oxidase and a NADPH-producing enzyme, glucose-6 phosphate dehydrogenase, are elevated in the fat tissues of obese mice, and they trigger local ROS accumulation and inflammation in adipose tissue (5, 51, 52). However, the molecular mechanism by which a local increase in oxidative stress in the fat tissues could bring about a systemic increase in the ROS accumulation in obesity remains unclear.

In this study, we demonstrated that the prooxidative conditions such as hypoxia and inflammation could reduce adipose GPx3 expression and, thereby, contribute to the decreased plasma GPx activity. As a major antioxidant enzyme in circulation, reduced plasma GPx3 level has been shown to be associated with enhanced systemic oxidative stress to increase susceptibility to childhood idiopathic stroke (53, 54),